Durability of High Density Polyethylene for Potable Hot Water Applications: Crack Propagation

A THESIS
SUBMITTED TO THE FACULTY OF
UNIVERSITY OF MINNESOTA
BY

Gyanender P. Singh

IN PARTIAL FULFILLMENT OF THE REQUIREMENTS
FOR THE DEGREE OF
MASTER OF SCIENCE IN MECHANICAL ENGINEERING

Dr. Susan Mantell, Dr. Jane Davidson

September, 2012

Acknowledgements

I am indebted to my adviser Dr. Susan Mantell for giving me the opportunity to work on this project. The numerous hours she spent discussing with me many interesting aspects of this project not only helped me in the thesis work but also improved my approach towards research. I am grateful to my co-adviser Dr. Jane Davidson for her questions which made me think deeply and improved the overall quality of this work.

I am thankful to my lab mates Stephanie King, John Korkko, Samuel Kim, Dongwon Lim, Casey Briscoe, Emily Paukert, Clayton Fitzgerald, and Matt Churchill who have either directly contributed to this project or have provided valuable suggestions for this project problem. Special thanks to graduate student Michael Slotman for helping me with the MTS tensile test machine.

I would like to acknowledge Mr. Dave Hultman for making the gripping system, precise crack forming device and helping with the installation of the heater used in this project. I would also like to thank Chevron Phillips Chemical Company for providing funding for this work.

Also, I am grateful to my family, particularly my parents, for contributing to my education and supporting me throughout my life.

Abstract

Polyethylene (PE) pipes, are used for water delivery, are susceptible to oxidation. As a result of oxidation PE becomes brittle and brittle pipes/tubes crack under the influence of tensile loads. These cracks initially propagate slowly and later on grow quickly becoming unstable. The focus of this study is slow crack growth in high density polyethylene (HDPE). Crack propagation experiments were conducted to determine the dependence of crack growth on degradation and stress levels.

HDPE samples, with 0.3mm thickness, were exposed to 80°C chlorinated water (5-8 ppm) for up to 65 days. Thin samples were selected to ensure uniform degradation through the thickness. Although the brittleness of the polymer can be evaluated using strain-at-failure, the drawback of this method is that it destroys the sample. The Carbonyl Index (CI) obtained by Fourier Transform Infrared (FTIR) spectroscopy was established as a nondestructive measure of the degradation level. CI ranged from 35 to 93. A higher value of carbonyl index represents a greater extent of degradation. The relationship between CI and loss of mechanical performance was validated by strain-at-failure. Crack propagation tests were conducted were conducted on degraded polymer samples at constant load. The load (stress level) ranged from 5.1 to 9.2 MPa. In all 5 samples were tested. It was found that the crack propagation rate ranged from 6.31×10^{-10} to 1.26×10^{-2} m/s while the stress intensity factor ranged from 0.91 to 4.07 MPa$\sqrt{m}$.

For a single degradation level, regardless of stress, the data when converted to log scale, and fit with the linear elastic fracture mechanics (LEFM) relationship $\frac{da}{dt} = CK^n$. As the degradation increased the crack propagation rate increased such that all data were fit by the relationship $\frac{da}{dt} = C(CI)K^n$ such that the exponential parameter 'n' was a constant for all the samples regardless of the level of degradation. The LEFM model fit to the data was best for moderate and high levels of degradation corresponding to CI of 55 and 90. Scanning Electron Microscopy (SEM) images show minimal deformation in the region around the crack tip, and ductile fibril stretching in the process zone. While the polymer had become brittle upon oxidation, there is local ductility in the process zone. An LEFM approach is typically applied to brittle materials, while the SEM results show that crack propagation is a combination of brittle and ductile behavior. Future studies should consider other modeling approaches that allow for ductile behavior in the process zone.

Table of Contents

List of Tables

List of Figures

Nomenclature

σ_i: hoop stress

σ: stress

a: crack length

CI: Carbonyl index

COD: crack opening displacement

K: stress intensity factor

N: number of load cycles

Q: activation energy

R: ratio of minimum to maximum load in cyclic fatigue test

R_{CG}: resistance to crack growth

R: Universal gas constant

r: resistance of the resin to slow crack growth

SDR: standard diameter ratio

t: time

t_{fi}: time to failure

T: temperature

Y: geometric factor

1. INTRODUCTION

1.1 POLYETHYLENE PIPE APPLICATION

Since the 1960s, polyethylene (PE) has been used for water piping applications worldwide [1]. About 350,000 miles of plastic pipes are used in USA and PE piping constitutes a major portion of it. More than 80% of the newly installed pipes used for transportation and distribution of natural gas use polyethylene [2]. In total, over 20,000 miles of PE pipe is installed every year [3].

1.2 IMPORTANCE OF SLOW CRACK GROWTH

Pressure rating (PR), resistance to slow crack growth (SCG), and resistance to rapid crack propagation (RCP) are three important attributes used to evaluate the performance of plastic piping materials [1]. Slow crack growth is responsible for most of the failures in pressurized polyethylene pipes during field application [2]. Stress concentrations serve as initiation locations for cracks which ultimately lead to failure. Such stress concentrations in the form of notches may be created at the external surface of the pipes during their installation [4]. However, for water transportation applications, in which chlorine is used as a disinfectant, chemical degradation occurs at the inner surface of the pipe where cracks develop under the action of water pressure. Hydrostatic design stress (HDS) (ASTM D 2241) is the maximum tensile stress in the wall of a pipe

in the circumferential direction due to the internal hydrostatic water pressure. Continuous improvements in the pipe material have resulted in significant increases in the HDS. A higher HDS allows the water design engineer to increase the flow capacity in two different ways by increasing: (1) the pressure level or (2) the diameter ratio [1]. However, improvements in the material have posed challenges to testing the material for slow crack growth as the testing time has increased to practically difficult levels.

The study presented herein focuses on slow crack growth in high-density polyethylene (HDPE) pipes exposed to pressurized chlorinated hot water. Slow crack growth depends on several factors and most important of them are the chemical degradation extent and the stress level to which the polymer pipe is subjected.

1.3 RESEARCH OBJECTIVES AND APPROACH

The goal of this study is to understand the effect of chemical degradation and stress level on the crack propagation in HDPE tubes. Thin plaque samples were degraded to specific levels so as to represent different sections of the tube which is most degraded at the inner surface and least degraded at the outer surface. As the material degrades, it becomes brittle. The material fails at low strain levels. Thus, strain at failure is one mechanical measure of the extent of degradation. Strain-at-failure can be measured by a tensile test. The fundamental drawback of this method is that the sample is destroyed and is no longer fit for use in crack propagation tests. Fourier Transform Infrared (FTIR)

Spectroscopy is a nondestructive alternative for evaluating the degradation level of the polymer sample.

Crack propagation tests, focused on measuring crack length as a function of time, were conducted on degraded HDPE samples. The results illustrate the effect of stress levels and degradation on crack propagation behavior. Scanning Electron Microscopy (SEM) was also conducted on samples that had been used in the crack propagation tests. The SEM images provided insights into the mechanism of failure of polymer tubes through slow crack propagation.

2. LITERATURE REVIEW

2.1 SLOW CRACK GROWTH

The performance envelop of PE, represented by log stress vs. log time, can be divided into three stages depending upon the governing mechanism of ageing [5]. In stage 1the material degrades by undergoing visco-elastic creep. Plastic pipes are designed for pressure levels which induce stresses that are much lower than the yield strength of plastic material; therefore, ductile failures are not observed in plastic pipes.

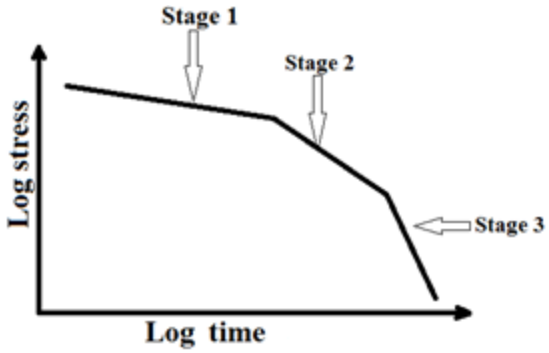

Figure 2.1: Different stages during the ageing of plastic pipes [5]

In stage 2 failure of the material happens due to brittle fracture. The time to failure, belonging to this stage, can be divided into two parts: crack initiation time and slow crack growth [6]. The PENT (Pennsylvania Edge Notch Tensile) test is a standard

test used to make sure that the material is strong enough to resist slow crack propagation, which is a common feature of this stage [5]. Unlike stages 1 and 2, in which mechanical loads are responsible for the failure of the material, stage 3 represents the failure of the material due to combined action of chemical agents (oxidizing agents) and mechanical loads. In the failures belonging to this stage, the mechanical loads are lowest and failure times are longest of all the stages. In the work presented herein, the failures of polyethylene belonging to the stage 2 and stage 3 have been studied and an attempt to predict the lifetime, when the failure belongs to one of these stages, has been made.

2.2 STANDARD TESTS

Several methods have been developed to predict the long-term performance of polymer pipes. Many of these methods are empirical. The Standard Extrapolation Method is used for predicting the long-term performance of plastic pipe according to ISO/TR 9080 standard [7]. The method is based on regression and involves four constants and two independent variables: temperature and hoop stress. These constants and variables are used in the equation which gives the time to failure as:

$$\log(t_{fi}) = -A - (B/T_i)\log(\sigma_i) + C/T_i + D\log(\sigma_i). \qquad (2.1)$$

The method has two models depending upon whether the regression coefficient D is zero or not.

The Rate Process method is another empirical approach used in the plastic pipe industry for forecasting the long–term performance of polyethylene pipes [8]. The method uses an empirical relation between time to failure, the stress level and the temperature. The three constants are empirically determined. . The method is valid only for applications in which the failure modes are the same as the field tests. Also, the method is geometry specific i.e., one set of constants in the extrapolation equation for a particular geometry are not applicable to the other geometry.

Although these methods have been successful to a certain extent in predicting the lifetime of polymer tubes, due to being purely empirical the applicability of these methods is limited to specific cases. An alternative approach is to predict the total time of several stages of failure to obtain the total lifetime of the tube. Slow crack growth is one of the stages of pipe failure and resistance of the material to slow crack growth is a very important attribute. The pipe material designation code according to ASTM standards is PE ABCD where digit A is related to the base resin density, digit B is related to the slow crack growth, and the third and fourth digits: C and D are related to the hydrostatic design stresses [1]. For example, PE 3408 is a polyethylene with density cell class of 3, slow crack growth class of 4 and HDS of 800 psi (last two digits are obtained by dividing the HDS by 100).

The creep rupture test is a standard test used for determining the design stress and the service lifetime of the polyethylene. In this test a length of the pipe is pressurized with a gas or liquid and its failure time is noted. The test follows the ASTM D1598

standard and is useful for establishing the relationship between the stress level and the life time of the tube [9].

A more popular standard test used to measure the resistance of polyethylene material to slow crack growth is the Pennsylvania Edge–Notch Tensile Test (PENT; ASTM F1473) [2]. The test is generally conducted at the accelerated conditions of 80 °C, with a sharp notch [10], and at 2.4 MPa stress which is much less than the yield strength (26-33 MPa). A typical PENT test specimen is in rectangular shape with small thickness and notched on its side. However, temperatures lower than 80 °C and stresses lower than 2.4 MPa can also be used to carry out the test. The failure of the sample is defined as the complete separation of the two halves of the specimen or the occurrence of extensive deformation in the remaining ligament [2]. Although the test is used by pipe manufacturers to rate the resistance of polyethylene towards slow crack propagation, some researchers have questioned the correctness of the method on the basis of lack of correlation found between the PENT test and the creep rupture test. For example, Krishnaswamy et al. [2] conducted creep rupture tests on two brittle high-performance PE4710 pressure rated pipes (HDPE-A and HDPE-D). The data were obtained for hoop stress vs. failure time and it was found that the HDPE–D was more resistant to slow crack propagation than HDPE–A. The authors also conducted PENT test for several PE pipe samples of the same materials at the same temperature (80 °C) which indicated that, contrary to the creep rupture tests, HDPE–A had longer failure time than HDPE–D polymer samples. The authors showed through experimental work that towards the end of

the PENT test, the failure of the samples took place due to ductile failure (post yield tensile stretching) during which the fibrils connecting the two halves of the sample were completely stretched and ultimately broken. This failure mechanism of PENT test samples was different from that found in the failure of brittle pipes in which the material does not deform appreciably before breaking**.** It was concluded that because of the differences in the mechanism of material failure, the PENT test does not correlate well with the brittle failure of polyethylene pipes.

Another test used for characterizing the resistance of polyethylene pipes to slow crack growth is the notched pipe test [11]. The test method follows ISO 13479:2009. The maximum thickness of the pipe that can be tested is 5 mm. Before the recent modifications, this test was conducted according to ISO 13479:1997 standard [12] in which four equi-spaced longitudinal notches are made on the outer surface of the pipe using the V-edged cutter. The testing environment is according to the ISO 1167 and EN 921 standards [13]. The test is conducted at 80°C so as to accelerate the crack growth rate. The pipe is subjected to hydrostatic pressure which depends on its SDR. The resistance to slow crack growth is expressed in terms of the time to failure [12] [13].

Pinter et al. [14] employed a different approach for characterizing slow crack growth. The proposed concept uses a special cracked round bar specimen (CRB) and fatigue tests to accelerate the crack growth. Firstly, the different S-N (log stress vs. number of cycles) curves for different R ratios (minimum load / maximum load) are obtained by performing cyclic fatigue tests on CRB specimens. The data are converted to

"synthetic" FCG (fatigue crack growth) curves, log da/dt vs. log K_{max} (a, t and K_{max} denote crack length, time and maximum stress intensity factor), using fracture mechanics computational concepts. From these FCG curves, log K_{max} vs. R_{CG} curves (R_{CG} donote the resistance to crack growth in terms of energy required for crack propagation) are generated for different crack growth rates. These curves are then extrapolated to R = 1 which corresponds to static loading. The extrapolated data were used to obtain the "synthetic" CCG (creep crack growth) curves. In this approach, a direct measurement of the rate of crack growth with the number of cycles (da/dN) is difficult [15]. Frank et al. [6] have proposed a method for measuring da/dt indirectly by measuring the specimen compliance, which is defined as COD/F where COD is the crack opening displacement and F is the applied load.

2.3 MODELS AND THEORIES

Choi et al. [16] proposed a model for crack propagation in polyethylene based on Crack Layer Theory [17] which explains the step-wise crack growth in polyethylene subjected to both mechanical and chemical degradation. The model considers the existence of a process zone. The process zone is a region of large localized deformation present just ahead of the crack tip as shown in Figure 2.2.

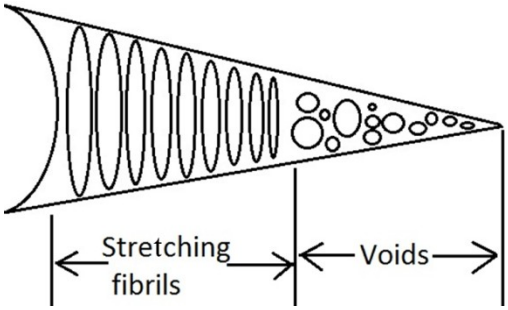

Figure 2.2: Schematic diagram showing voids and fiber stretching in the process zone (modified from [16])

The crack and the process zone are jointly referred to as the crack layer. The movement of the crack and process zone is mutually interdependent and based on the energy absorbed/released during the progress of the crack layer. The driving force for crack growth and process zone evolution are defined as $X^{CR} = (J_1^{CR} - 2\gamma)$ and $X^{PZ} = (J_1^{PZ} - \gamma_c)$ respectively where X^{PZ} and X^{CR} are the thermodynamic forces for process zone evolution and crack growth respectively, J_1^{PZ} is the energy release rate (ERR) due to the process zone front movement, J_1^{CR} is the ERR due to the crack growth, γ_c is the specific energy of crazing, and 2γ is the specific fracture energy of the cold drawn material. The proposed kinetic equations for crack and PZ growth are:

$$\frac{dc}{dt} = X^{CR} \qquad (2.2)$$

$$\frac{dL}{dt} = X^{PZ} \qquad (2.3)$$

where ‘c’ and ‘L’ are the crack length and the sum of crack length and process zone respectively. The failure mechanism of the polymer is not thoroughly presented by the authors but simultaneous degradation along with crack growth is considered.

Brown et al. [18] proposed a theory for crack growth in polyethylene which relates the crack opening displacement rate with several factors including the yield point of polymer, stress intensity factor, intrinsic viscosity of fibrils in the craze, and Young's Modulus. Brown [4] asserts that for linear polyethylene (substantially short-linear chains of polyethylene) structures the failure time due to slow crack growth is dependent upon five factors: resistance of the resin to slow crack growth (SCG) (R_{CG}), size of the defect responsible for crack growth (a), geometric factor (Y) which is dependent on the ratio of size of defect to specimen dimension, global stresses (σ) which also include the residual stresses, and the absolute temperature (T). In his work with Lu [19] Brown shows that the time to failure is related to these factors as $t = rK^{-n}\exp(Q/\boldsymbol{R}T)$ where K (the stress intensity factor) = $Y\sigma a^{1/2}$. The authors have stated that the constant n depends on the resin. The resistance of the resin to SCG can be measured using the standard PENT test. However, it should be made sure that the PE sample for which this theory is applied and the PE sample for which the PENT test is done are from the same lot so that they have the same microstructure. Using the above mentioned relation ($t = rK^{-n}\exp(Q/\boldsymbol{R}T)$) the authors investigated the effect of notch depth on the lifetime of pressurized pipes and developed a methodology to determine whether to discard the pipe or use the pipe depending upon the notch depth. However, they did not consider the effect of chemical degradation.

Lundback [20] proposed an empirical approach for predicting the lifetime of the polyolefin (polymer produced from simple pipe. Using Differential Scanning

Calorimetry, OIT (oxidation induction time) data were obtained for different depths in the pipe which was 2 mm thick. Using the data it was found that at the time of pipe failure the chlorine front reached a depth of 0.5 mm. The failure time of the pipe was then extrapolated from the OIT data at a depth of 0.5 mm at different exposure times. This approach is very specific because for pipes with different geometries (thickness, SDR) the chlorine front will reach different depths in the pipe at the time of pipe failure.

2.4 EXPERIMENTAL WORK

Several experimental studies focused on the long-term performance of polymer pipes have been conducted. Dear et al. [21] conducted hydrostatic pressure tests on Medium Density Polyethylene (MDPE) pipes having diameter 90mm with SDR 11 and 17.6. The pipes were pressurized with chlorinated water and were immersed inside a water bath (un-chlorinated) at 80°C. The chlorine concentration inside the pipes varied between 0.5 to 120 g/l and the hoop stress was kept at 4.6, 3.1, 2.7 and 0 MPa. The results indicated that the failure time decreased as the chlorine concentration and the stress level increased. The concentration of chlorine for this study was much higher than that for general potable water applications (2-5 ppm). Also, such hydrostatic tests are very expensive and time-consuming.

It has been observed that the crack growth in PE is not continuous but is stepwise. Lu et al. [22] performed constant load tensile tests on single edge-notched MDPE

specimens between 42°C and 80°C. Crack advancement was measured using an optical microscope. There were intervals of slow notch opening and crack advancement followed by rapid crack growth. The rate of increment in crack length, during quick crack growth, decreased with the decrease of the applied stress and temperature. Also, it was observed that below 3.2 MPa the failure was of ductile nature while above 3.9 MPa the failure turned brittle; however, the rapid increase in crack length could not be observed below 1.2 MPa.

As discussed earlier, several test methodologies have been developed to characterize slow crack growth in polymer and make lifetime prediction on its basis. Three point bending test, proposed originally by Leis et al. [23], is one such test and Kanninen et al. [3] examined its validity. Kanninen et al. have used a viscoelastic fracture mechanics approach to establish the transferability of LEFM (Linear Elastic Fracture Mechanics) based SCG data from the short-term laboratory tests to long-term service applications of PE pipes. The condition for transferability was found to be that the craze (intensely deformed inelastic zone) around the crack should be within the zone of dominance of LEFM crack tip fields. For those materials which satisfy the condition, the relation $da/dt = AK^n$ is applicable. In this relation, K is the stress intensity factor while A and n are empirical constants evaluated using the SCG data. Dear et al. [21] proposed a same crack growth relation for predicting the life time of PE tubes. However, these authors did not take into account the chemical degradation which occurs in plastics over time when exposed to corrosive environment.

Hamouda et al. [24] conducted an experimental study on medium density polyethylene (MDPE) and found a strong correlation between C^*, a creep load parameter, and time to failure. The authors conducted creep crack growth tests on full circumferential–notched rod specimens, double edge-notched bar specimens and tubes. The creep load parameter was dependent on several factors including load, load-point displacement rate, crack length and half specimen width. As mentioned in the previous section Brown [4] conducted experiments to investigate the effect of notch depth on lifetime of pressurized pipes and came up with a methodology to determine whether to discard the pipe or use the pipe depending upon the notch depth.

Trankner et al. [25] conducted an experimental study on medium and high density polyethylene to study the resistance to slow crack growth. Samples were machined from the pipe wall. The specimens were 25 mm x 8 mm in cross section and had 3mm notch depth with 1 mm side notches. These specimens were loaded uni-axially in tension at the temperature of 80°C. Through the test, large differences in the slow crack growth resistance between the materials were found. In principle, the test conducted in the study is similar to the PENT test which is a standard test used by researchers to assess the crack growth resistance of polymers. But samples for the PENT test are quite thick and it would take a lot of time to degrade them by chemical means. Lundback [20] conducted hydrostatic pressure testing of polyolefin pipes exposed to chlorinated water at the inside surface and to air at the outer surface at elevated temperatures of 95°C, 105°C, and 115°C. The chlorine concentration was controlled through loop circulation. It was found

that the fracture always initiated at the inner surface of the pipe which showed large number of cracks. The authors inferred that the inner surface of the pipe turned brittle due to chemical degradation followed by fracture initiation. The data presented shows that as the hoop stress decreased the pipe failure time increased. It also indicated that with the increase in temperature from 95°C to 115°C, the stress level required to cause failure decreased while the failure time increased. Besides these results, it was found that even a small amount of increase in chlorine concentration (0 to 0.5 ppm) caused an appreciable reduction in the failure time. However, with a further increase in chlorine concentration (0.5 ppm to 3 ppm), the failure time did not decrease much further.

Hingley et al. [26] performed fracture tests on three different types of polymers (two aromatic polyimides and one aromatic polyamide – imide). Using a razor notching procedure, a sharp notch was created in thin films of these materials which were 25 μm in thickness and 1.3 cm in width. The gauge length of the specimens was 5 cm. The specimens were subjected to displacement-controlled tensile tests with a cross-head speed of 0.185 cm min^{-1} and the crack propagation was observed with an optical microscope. A strong dependence of the crack initiation on the crack length was observed and the material obeyed the critical stress intensity criterion for crack initiation. Slow crack growth was observed along with the yield zone ahead of the crack tip. The yield zone was wider than the film thickness. Fracture toughness, which ranged between 1.65-5.4 $MPam^{1/2}$, was found to F depend upon film thickness as well as on the chemical nature of the polymer. Similar work has been performed by Klemann et al. [27].

Chan et al. [28] conducted three-point bend tests on high-density polyethylene single-notched specimens of different thickness(3, 6, 12 and 20 mm) in air, distilled water and detergent environment (Comprox 2740 and 98% distilled water by volume) at 19°C, 40°C, 60°C and 75°C. The specimens were loaded by applying a dead load. It was established that the critical stress intensity factor is the controlling parameter for crack growth in the material. The mechanism of failure was also postulated based on the SEM results.

As stated earlier, slow crack growth is responsible for the majority of failures occurring in pipe applications and some standard tests are available which can be used to quantify the resistance of the material to slow crack growth. For potable water applications the water flowing through the pipe contains chlorine as disinfectant which acts as an oxidizing agent. Due to the oxidizing action of chlorine, the polymer becomes brittle and cracks develop at the inner surface of the pipe. When these cracks propagate, their growth is influenced not only by the stress level which the pipe is subjected to but also the chlorine concentration and the exposure time to chlorine since the resulting degradation makes the material brittle and thus assists in crack propagation. None of the available standard tests takes into account these factors. At room temperature, any attempt to subject the test samples to chemical degradation simultaneously with mechanical loading in order to duplicate the actual practical condition increases the testing time several times. Although at elevated temperatures, which are commonly employed to accelerate the test, the reaction between polymer and the corrosive

environment will be speeded up but it may not be possible to accurately estimate the rate of crack growth at lower temperatures from the data as separating out the influence of temperature rise on chemical degradation from that on mechanical degradation (or change in mechanical properties of polymer) will be required and not enough knowledge base is available at present in this regard. In the present work we propose an alternative strategy to characterize the polymer degradation by simultaneously considering the effect of chemical degradation along mechanical loads.

3. EXPERIMENTAL PROCEDURE

The first step of this study is to develop a repeatable method of quantifying the extent of degradation in polyolefin materials. Once samples have been degraded and the extent of degradation quantified then the rate of crack growth as a function of stress and extent of degradation can be evaluated. This chapter describes the procedure used to degrade the high-density polyethylene (HDPE) samples, the method used to evaluate the degradation extent of samples using Fourier Transform Infrared (FTIR) Spectroscopy, details of the crack propagation experiments, and the procedure for analyzing the crack propagation raw data. Table 3.1 lists the experiments conducted.

Table 3.1: List of experiments

Experiment	**Objective**
Degradation of HDPE samples in controlled environment	Prepare degraded HDPE sample for crack propagation tests
FTIR spectroscopy	Measure the extent of degradation of the HDPE samples
Tensile tests	1. Measure the strain at failure which is a mechanical method of measuring degradation 2. Validate the applicability of FTIR spectroscopy
Crack propagation tests	Understand the dependence of crack propagation rate on the load level and extent of degradation of HDPE
Scanning Electron Microscopy	Observe the surface of HDPE samples, used in crack propagation tests, in detail to understand the mechanism of failure

3.1 MATERIALS

The extent of degradation in polyolefins, exposed to an oxidative environment, will vary through the thickness. The greatest degradation will occur at the surfaces that are in contact with the oxidative environment [29]. For example, consider a tube with flowing hot potable water at the inner surface and air at the outer surface as shown in Figure 3.1. The cross section of the tube can be divided into regions with different levels of degradation D_1, D_2 and D_3, with $D_1 < D_2 < D_3$. To understand the effect of oxidation-induced mechanical degradation on the crack propagation rate, thin HDPE samples degraded to specific levels were prepared to represent these different regions of the tube as shown in Figure 3.1. Crack propagation tests were then conducted on the samples by subjecting them to tensile loads.

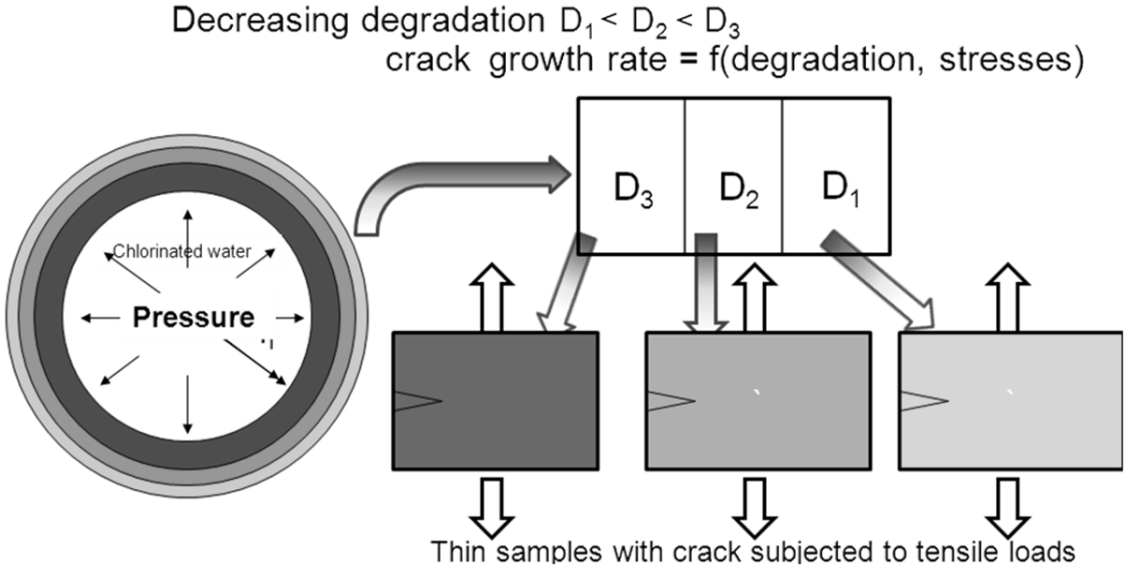

Figure 3.1: Different sections of the tube at different radii degraded to different extents D_1, D_2 and D_3.

The HDPE samples were obtained from the Chevron Phillips Chemical Company. The polymers were of two types based upon the type of antioxidant system present in the samples: 8C samples which contained 2000 ppm Irganox 1010 and 9C samples which contained 1000 ppm Irganox 1010 and 1000 ppm Irgafos 168. The polymer samples were in the shape of rectangular thin plaques with the dimensions as 0.03 cm (thickness) x 3.2 cm (width) x 4.4 cm (length).

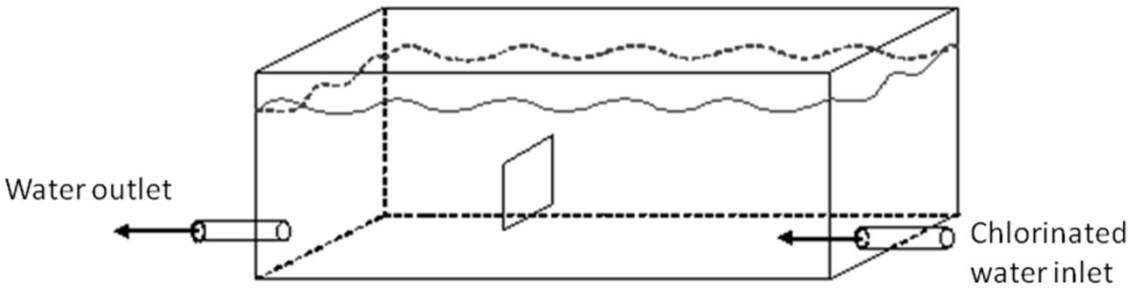

Figure 3.2: Thin plaque sample immersed in chlorinated-hot water tank

3.2 DEGRADATION PROCEDURE

Samples were degraded by immersion in a 80°C water bath (see Figure 3.2) in which the chlorine concentration was controlled to be at 8 ppm, pH is controlled to be within 6.8 ± 0.2 and the ORP (oxidation reduction potential) ranged from 700 - 750 mV. The samples were exposed to chlorinated water for up to 50 days. The water bath and control system are described in detail in [30]. The test apparatus, used for sample

degradation, is shown in Figure 3.3. The following is a brief summary of the key features of this apparatus.

The water bath is a 26.5 liter stainless steel bath equipped with a water level control system, heater/temperature controller, and a circulator. The bath is filled with reverse osmosis water. Bath chlorine and pH conditions are controlled and continuously monitored by a specially developed LabView virtual instrument. This data acquisition and control system is comprised of several sensors and electronically actuated (solenoid) valves. The desired chlorine set point is obtained by delivering a concentrated chlorine solution to the bath. Similarly the pH can be adjusted by adding a basic solution. The data acquisition and control software allows the user to achieve the desired free chlroine and pH set points by adjusting the duty cycle (both duration and frequency) of the electronic valves (that deliver the concentrated solutions). Chlorine, pH, ORP and temperature data are continuously recorded via the Labview data acquisition system. In addition, these bath conditions will be verified daily by manual measurements to ensure that sensor calibration is accurate.

Specific details regarding the water bath and control system are as follows. To maintain constant chlorine content, the free chlorine level in the bath is monitored by an FCLi system from Rosemount Analytical. The chlorine concentration data are acquired and interpreted by the LabView virtual instrument. To maintain the chlorine concentration set point, the LabView system actuates a solenoid valve to deliver a concentrated chlorine solution ($Ca(ClO)_2$ at approximately 275 ppm) into the bath as

necessary. Similarly, an AR125 Oakton 35108-00 controller interprets an AT125 Cole Parmer K-05998-30 pH sensor. The Oaktron controller sends pH data to the DAC (LabView), which cycles the solenoid valve to discharge a basic solution (Na_2CO_3) as necessary. The oxidation reduction potential (ORP) is monitored using an AT126 Cole Parmer K-27003-50 sensor. The ORP data are input to the data acquisition system: the ORP level is recorded, but not controlled. The Chromalox resistance heater is controlled by a separate Process Technology (model number HXL1108-R12-P1) temperature controller.

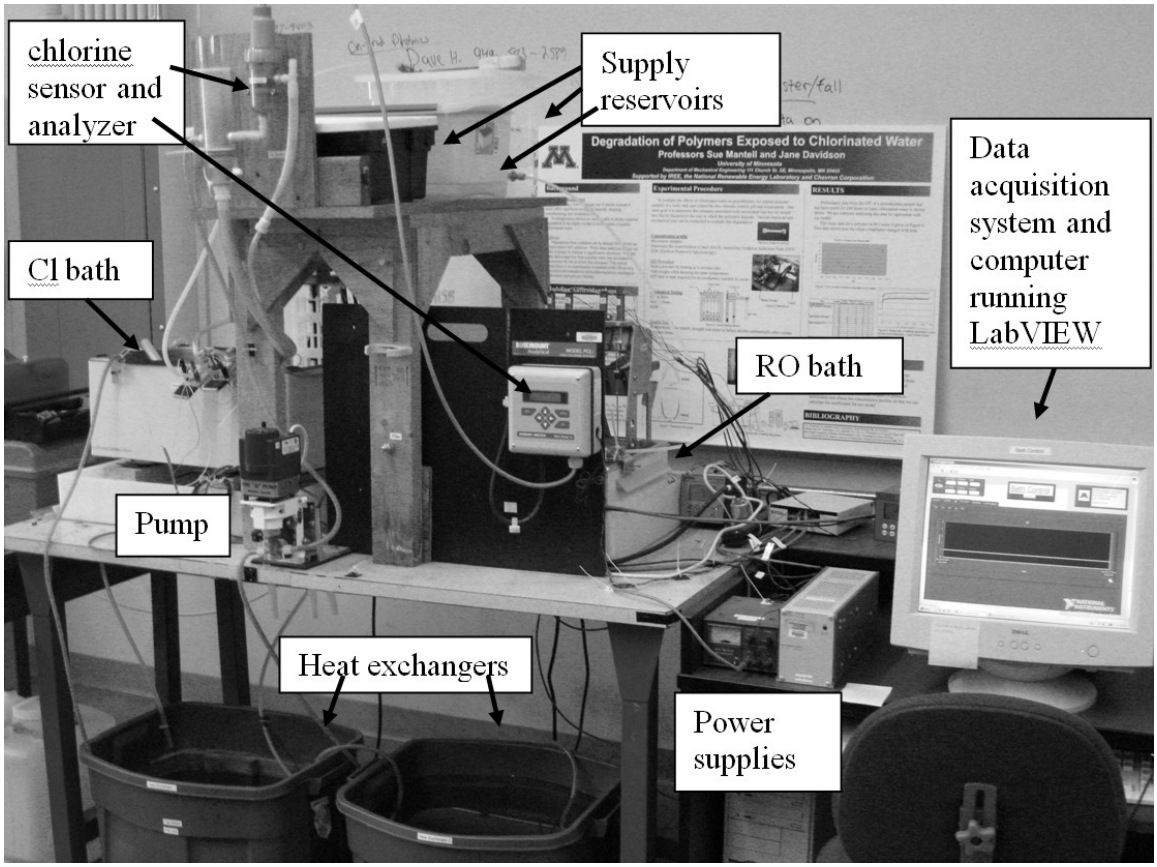

Figure 3.3: Photograph of test apparatus (source: [28])

3.3 MEASURING THE EXTENT OF DEGRADATION

As the polymer degrades due to the oxidizing action of the chlorine it loses toughness and becomes brittle. The crack propagation behavior of the polymer is dependent upon its brittleness. To study the dependence of crack propagation on the extent of degradation, samples having different extents of degradation were prepared.

A quantitative method to measure the extent of degradation was required. A common method to quantify toughness is to evaluate the area under the stress strain curve from the tensile test; the greater the area the tougher the material. A typical stress-strain curve for the polymer is shown in Figure 3.4. An increase in stress is required to elongate the sample until the yield point is reached. Beyond the yield point no further increment in stress is needed and the sample elongates until strain hardening begins. After the beginning of strain hardening, an increase in stress is again needed to elongate the sample further. This behavior continues until the ultimate tensile strength of the material is reached, at which point the sample breaks. Degradation reduced the ultimate stress and strain at failure. However, the yield point and the constant-stress elongation prior to strain hardening are not significantly affected by degradation. Therefore, the strain at failure can be used to evaluate degradation of the polymer. A drawback of this method is that, after tensile testing, the sample can no longer be used for crack propagation experiments. So, to evaluate both the extent of degradation and fracture behavior of the same sample, an alternative method to measure the extent of degradation is required.

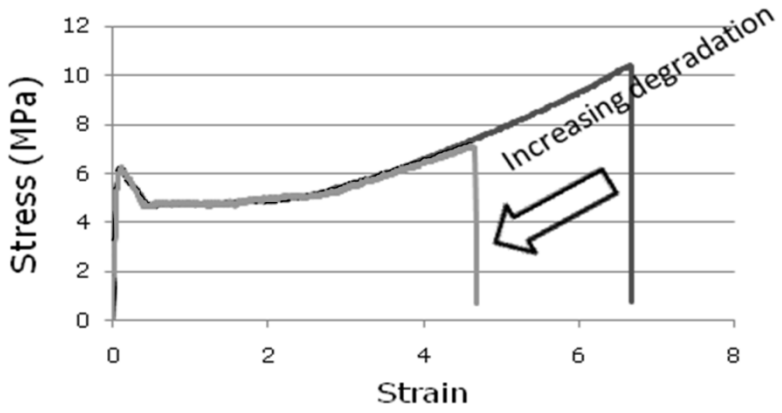

Figure 3.4: A typical stress strain curve for polyethylene

Fourier Transform Infrared (FTIR) Spectroscopy has been extensively used to determine the chemical composition of different substances. When polyethylene is oxidized, different products containing the carbonyl group (C=O) such as ketones, aldehydes and esters are formed. With an increase in the extent of oxidation, the amount of chemical species containing the carbonyl group also increases. Thus, the absorbance of infrared waves in the frequency range corresponding to carbonyl compounds can be used as a nondestructive measure of the degradation of the polymer.

The plots of absorbance vs. wave number were obtained with a Nicolet Magna-IR 750 spectrometer. The carbonyl absorption band in the infrared spectrum lies between 1690 cm^{-1} – 1790 cm^{-1} [16]. Therefore, to obtain the extent of oxidation, the area under the absorbance peak in the corresponding frequency range was evaluated using the Omnic software. The area was normalized with the absorbance value of the polyethylene (2018 cm^{-1}) group. The normalized area, referred to as the Carbonyl Index (CI), is a representation of the amount of carbonyl compound present in the degraded sample:

$$CI = \frac{\text{area under the peak corresponding to carbonyl compounds}}{\text{height of the peak corresponding to the polyethylene group}} \quad (3.1)$$

A larger CI corresponds to a higher quantity of carbonyl compound in the polymer which indicates greater degradation. Other researchers have defined similar carbonyl indices to quantify the oxidation products in polymers.

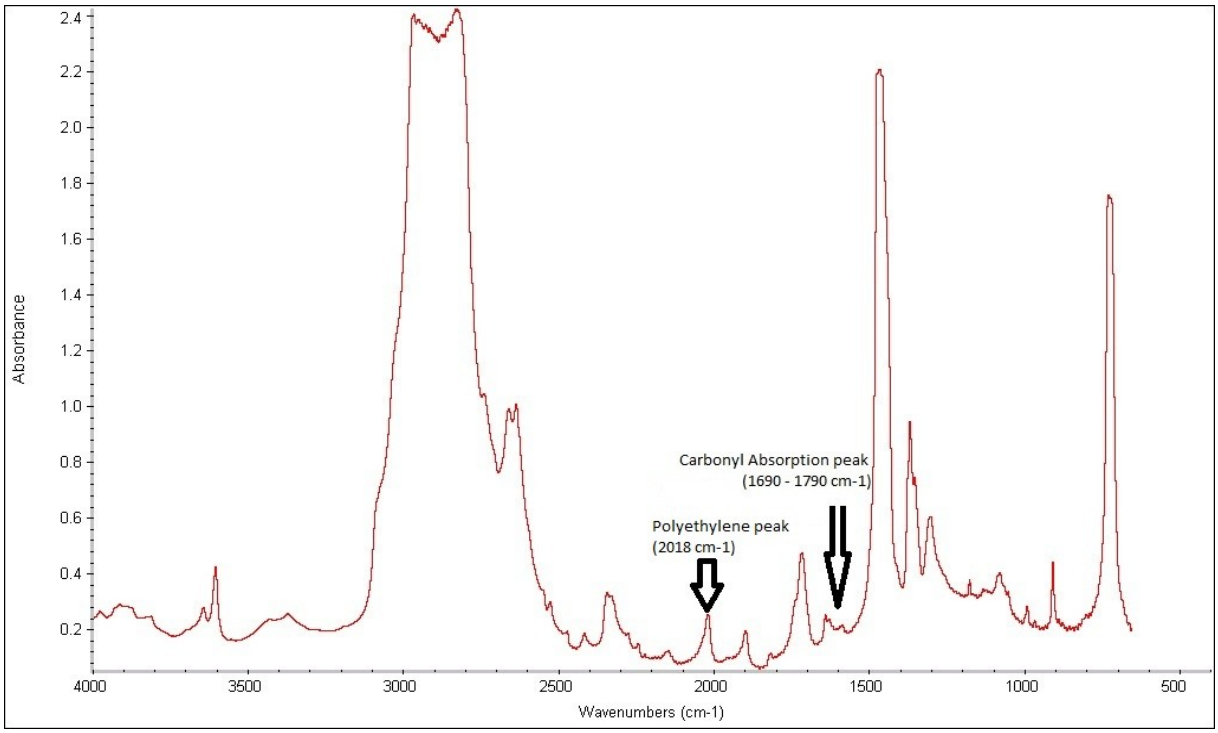

Figure 3.5: Infrared spectrum for a polymer film

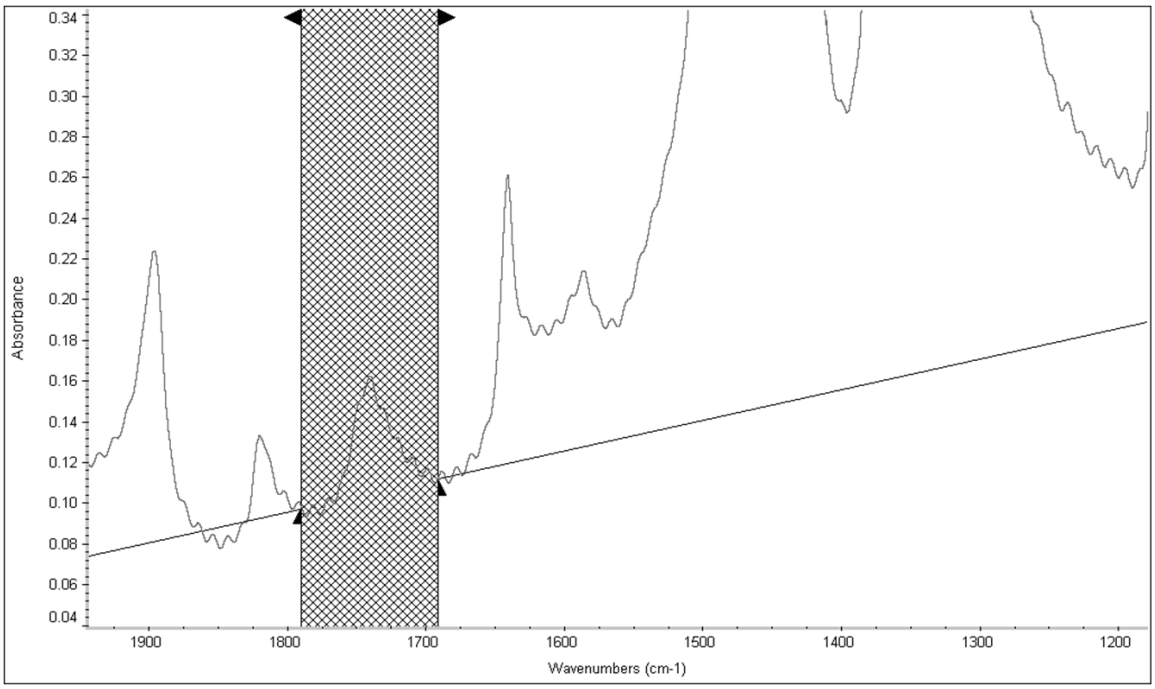

Figure 3.6: Measurement of area under the peak corresponding to the carbonyl compounds in the infrared spectrum

To explore the validity of FTIR as a quantitative measure of degradation, samples exposed to chlorinated water were evaluated by FTIR and subsequently tensile tested to failure. The Transmission Sampling technique on the Nicolet Magna-IR 750 spectrometer was used for finding the relative quantity of carbonyl compounds present in the polyethylene samples degraded to different extents. The velocity, aperture, gain, resolution and number of scans were set as 1.8988, 2, 2, 4 and 32 respectively. The tensile tests were conducted using a MTS QTest machine. The original rectangular thin plaque samples were cut into the dog bone shaped specimens using a die (ASTM 1708) from Pioneer Dietecs Corporation; see Figure 3.7. These dog bone shaped samples were then subjected to a constant strain rate of 0.2 in/min until fracture (Figure 3.8).

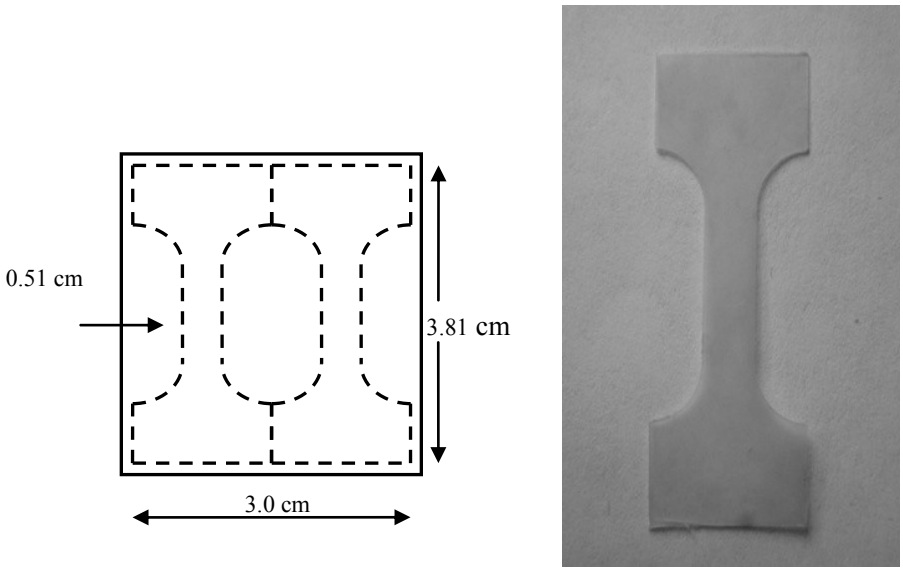

Figure 3.7: Schematic diagram with dimensions and a picture of dog bone shaped specimen cut from the plaque samples for tensile tests.

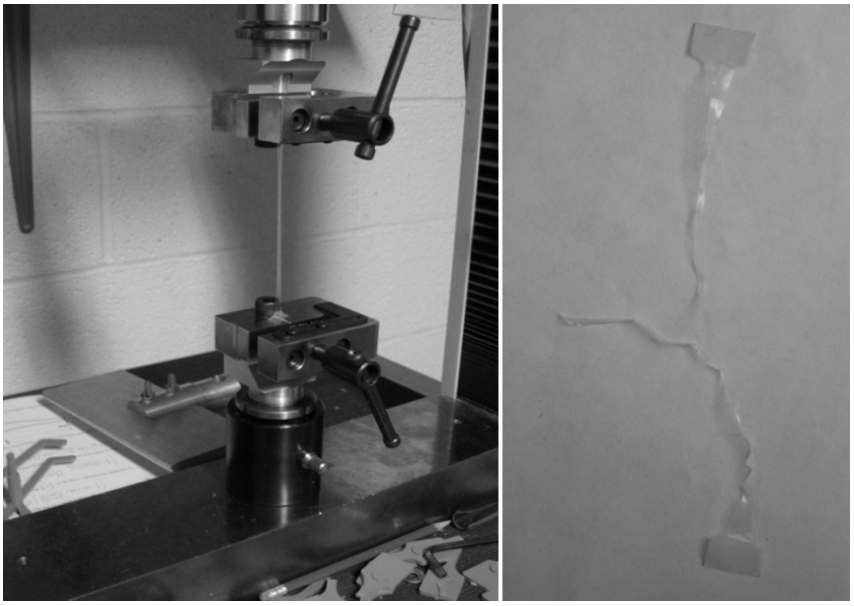

Figure 3.8: A strain-to-failure test being carried out on a MTS QTest machine, and the stretched sample after the test

The elongation vs. load data were converted to engineering strain vs. stress using the original dimensions of the specimen. The strain is the elongation per unit original length and stress is the load per unit original area. The FTIR data were then compared with the strain-to-failure test data to check the applicability of this spectroscopy method for evaluating the brittleness of the polymer. It will be shown in the 'Results' chapter that a good correlation existed between the FTIR and strain-to-failure test data. Thus, the applicability of the FTIR spectroscopy was established for characterizing the degradation of mechanical properties of thin HDPE films.

3.4 CRACK PROPAGATION

After analyzing the degraded polyethylene samples using FTIR, notches were introduced and crack growth experiments were conducted by subjecting the samples to constant tensile loads. The notches were made using a 0.2 mm thick X-ACTO knife. The initial crack lengths ranged from 4.2 mm to 7.0 mm. Each polyethylene specimen was loaded in tension on a BT Technologies load frame. The sample was mounted in the load frame via steel grips with sandpaper to reduce slippage. A dead load is transferred to the sample through a lever arm (Figure 3.9).

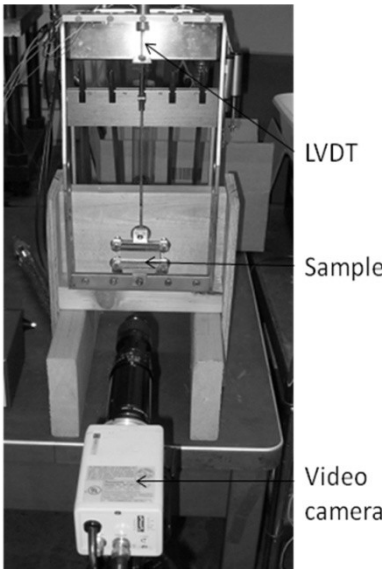

Figure 3.9: Crack propagation experimental set-up

The load frame was placed in front of the optical measurement system, as shown in Figure 3.10, which was used to record the crack growth in the sample. The measurement system included a Panasonic CCTV camera (WV-BP330), Navitar lens system, a tripod stand for holding the camera and lens system, a video capture card (HD 600 PCI Digital and Analog TV Tuner from ATI TV wonder), a computer with a video editing and processing software. The specimen was illuminated with a 100W light bulb. The Navitar lens system consisted of a 0.67X lens adapter (1-6020), 6.5X high-magnification zoom lens (1-60135), a 0.25X lens attachment (1-6044) and a C-mount coupler (1-6010). The recorded videos of crack propagation were broken down into images separated by regular intervals of time using a VLC media player, an open source player from VideoLAN organization. Each image was filtered based upon the pixel

intensity using MATLAB. The images available for processing had a resolution of 96 dpi.

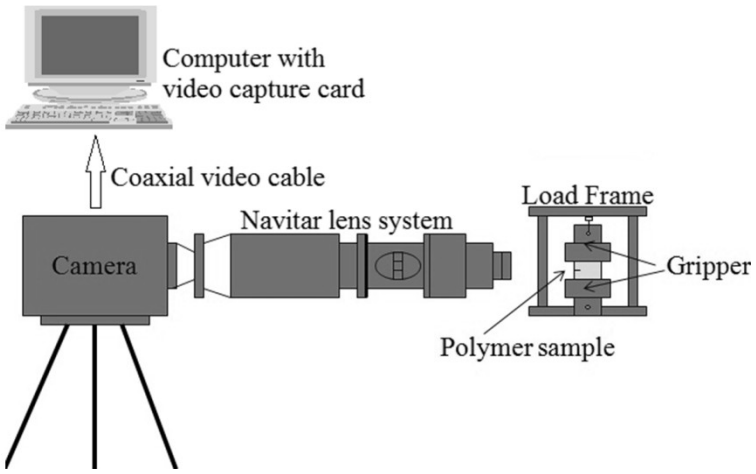

Figure 3.10: Schematic diagram showing crack propagation experiment set up with camera and polymer sample

3.5 DATA ANALYSIS

Images obtained from the crack propagation videos were processed to evaluate the respective length of the crack and process zone. Figure 3.11 shows such an image. The crack length (a) and process zone length (l) as functions of time (t) were evaluated. On the images, the crack tip was marked using a white line in Paint software (Figure 3.12). The image was then filtered in MATLAB to turn off the pixels (setting pixel intensity to be zero) with intensity below a threshold intensity; the intensity of pixels above the threshold was set as 1. One such image is shown in Figure 3.13. The total crack length, which also included the process zone length, was then found in terms of the

number of pixels in the filtered images using MATLAB Image Processing toolbox. A calibration factor was then used to convert the number of pixels to length.

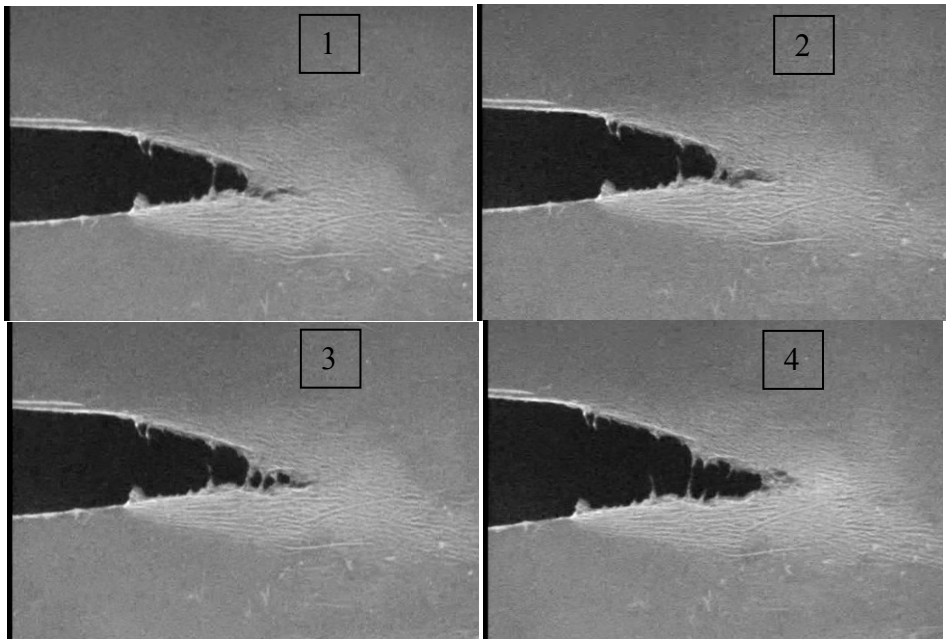

Figure 3.11: An image from a crack video showing the crack and process zone progression

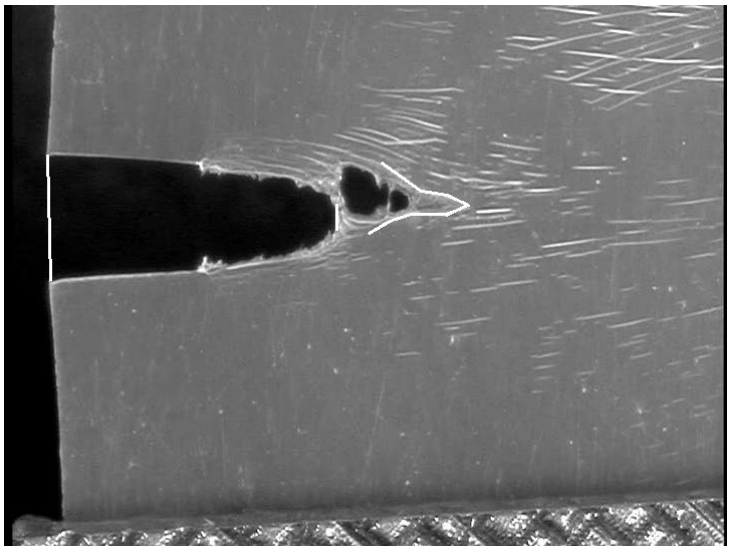

Figure 3.12: An image from a crack video showing the marking of the sample edge, crack edge and process zone edge in order to calculate the crack and process zone length

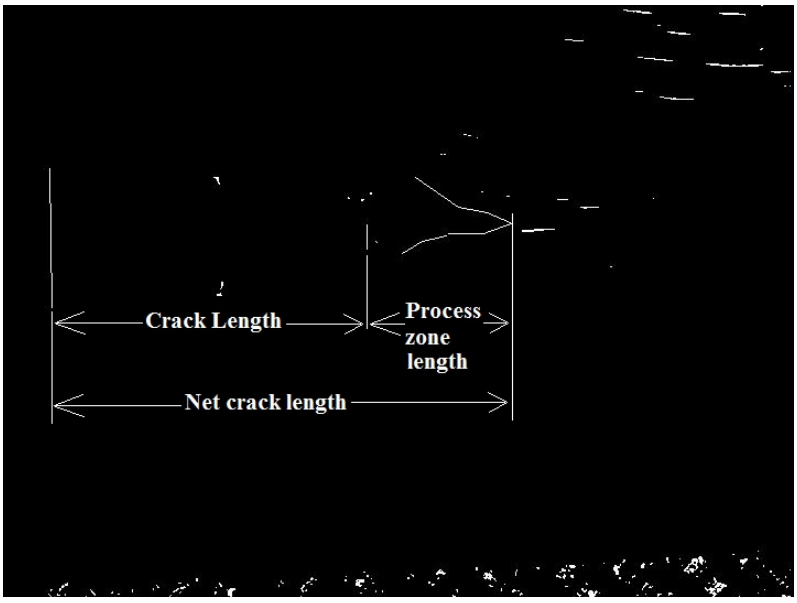

Figure 3.13: An image from crack video filtered in MATLAB showing different lengths

The crack propagation rate was assumed to follow the relation

$$\frac{da}{dt} = CK^n \quad . \qquad (3.2)$$

The stress intensity factor (K) is evaluated as a function of the geometry factor 'Y', remote stress 'σ' and the crack length 'a'

$$K = Y\sigma\sqrt{\Pi a} \quad . \qquad (3.3)$$

Substituting (3.3) into (3.2) and taking logs on both sides of the resulting equation gives

$$\log (da/dt) = \log (C) + n \log (Y\sigma\sqrt{\Pi a}) \quad . \qquad (3.4)$$

The crack propagation rate was evaluated at each time instant using the following numerical expression:

$$\left(\frac{\Delta a}{\Delta t}\right)_{t=t_i} = (a_{i+1} - a_i) / (t_{i+1} - t_i). \qquad (3.5)$$

To avoid numerical difficulties, inaccurate crack length measurements that produced negative crack propagation rates, especially in the early periods of crack advancement, were by-passed in the numerical calculation.

4. RESULTS

The results from this study can be divided into two broad categories: 1) relationship between FTIR spectroscopy and tensile test results and 2) Crack propagation test results.

4.1 FTIR SPECTROSCOPY AND TENSILE TESTS

Four 8C samples, which contained 2000 ppm Irganox 1010, and five 9C samples, which contained 1000 ppm Irganox 1010 and 1000 ppm Irgafos 168, were exposed to 8 ppm hot chlorinated water at 80°C. The test apparatus for material degradation was operated continuously for 50 days. At different intervals of time (listed in Table 4.1) polymer samples were removed from the water bath and their FTIR spectroscopy data were obtained. After recording the FTIR data, dog bone shaped specimens (ASTM 1708) were cut from these PE films using a die (see section 3.3 for details) and tested in tension until failure.

The data from FTIR spectroscopy and tensile tests are shown in Table 4.1. Due to exposure to the oxidative environment the polyethylene chain broke and carbonyl compounds were formed. Consequently, the quantity of the carbonyl compound increased with the exposure time and resulted in a higher carbonyl index. The mechanical properties of the polyethylene also degraded due to oxidation, resulting in increased brittleness and reduced strain–at–failure.

Table 4.1: FTIR Spectroscopy and tensile tests data

Exposure time (days)	1.5	3	5.5	8.5	12.5	19.5	24	35	45
Carbonyl Index (CI)	6.6	3.4	5.4	4.0	6.6	8.3	16.3	41.4	53.6
Strain-at-failure	6.73	6.54	7.16	5.31	6.23	1.03	1.20	0.33	0.15

Figure 4.1 shows the variation of strain–at–failure with the exposure time. For exposure time less than 12.5 days, there was no appreciable variation; strain–at–failure of the samples decreased from 6.73 to 6.23. There was a sharp decrease in the strain–at–failure from 6.23 to 0.15 for experimental time between 12.5 and 45 days. At that time, the strain-at-failure had become almost equal to zero and the material had lost much of its deformation ability. Figure 4.2 shows the variation of carbonyl index with the exposure time. For exposure time less than 12.5 days there was no appreciable change in the carbonyl index; it remained almost constant at 6.6. But thereafter a rapid increase in the carbonyl index from 6.6 to 53.6 was observed.

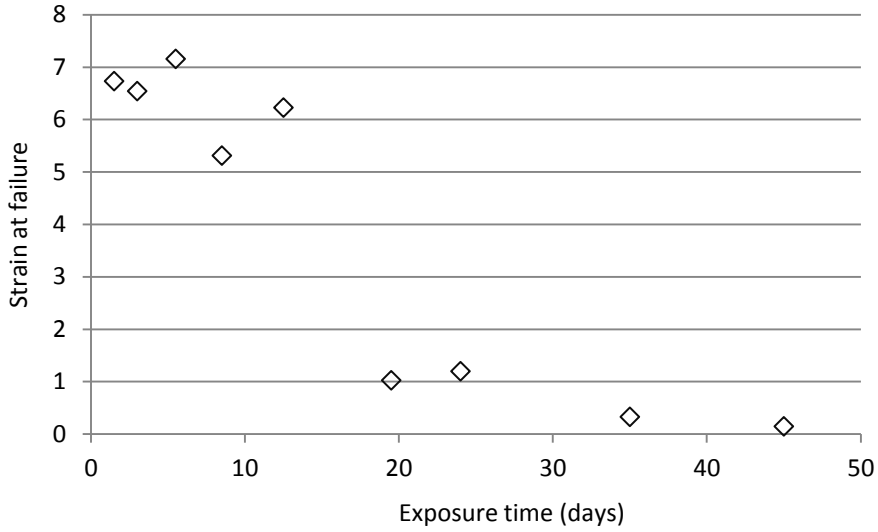

Figure 4.1: Strain-at-failure data for the HDPE samples exposed to 8ppm Cl water

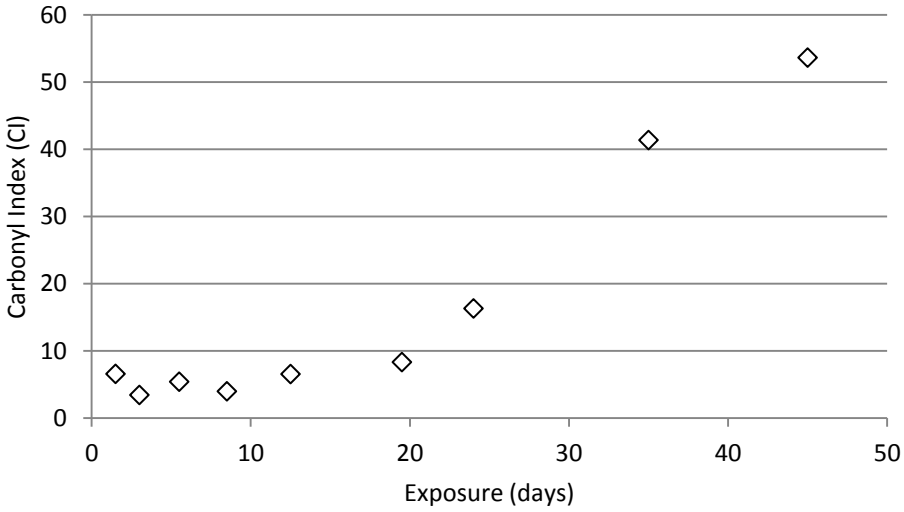

Figure 4.2: FTIR data for the HDPE samples exposed to 8ppm Cl water

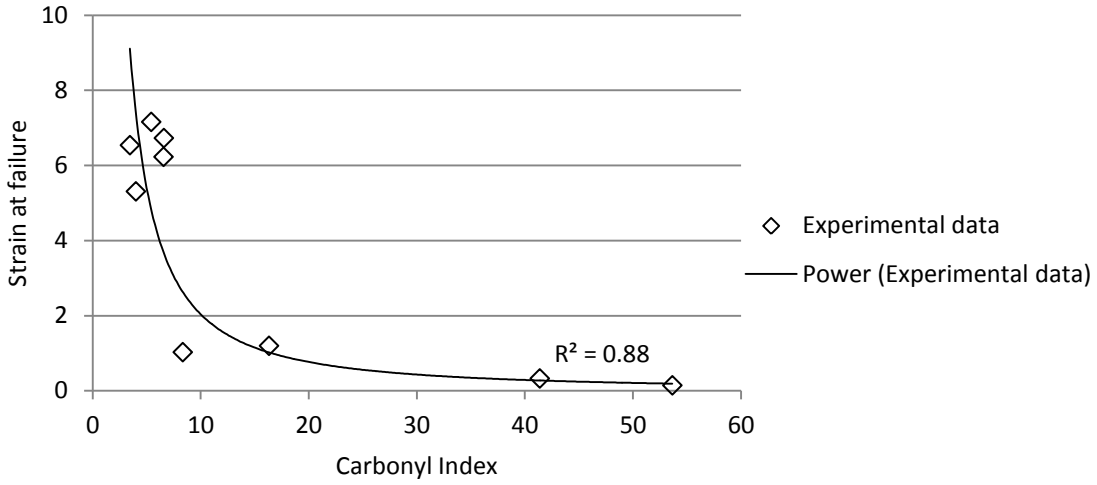

Figure 4.3: FTIR spectroscopy vs. strain-at-failure data for the HDPE samples exposed to 8ppm Cl water

The CI vs. strain-at-failure data were fitted to a power series function line as shown in Figure 4.3. It was found that a strong R squared value of 0.88 existed between FTIR spectroscopy data (CI) and the strain–at–failure values of the tested samples. A difference in the dependence of strain-at-failure and CI of polymer samples on exposure time is that the CI continued to increase with exposure time whereas the strain-at-failure did not continue to decrease. This result indicates that FTIR may be a more sensitive measure of degradation than the strain-at-failure. Figure 4.3 shows the relation between the strain at failure and the carbonyl index. A power curve is fitted to the data with a R squared value of 0.88. The curve is non linear and indicates an inverse relation between the strain at failure and carbonyl index.

4.2 CRACK PROPAGATION RESULTS

The samples, prepared by degradation using chlorinated water, were used for crack propagation experiments. An initial crack was created in the samples and a constant load was applied to the samples using the loading station as discussed in chapter 3. The extent of degradation (CI), stress level to which the sample is subjected and the initial crack length (normalized by the sample width) are listed for each sample in Table 4.2. The width of the samples used for crack tests was 32 mm. The Carbonyl Index ranges from 44 to 93. CI 44 corresponds to the sample which has begun to turn brittle while CI 93 corresponds to the sample which is very degraded and thus has lost almost all of its ability to deform. The tensile strength of the HDPE material used for this work is 17.2 MPa. In crack propagation experiments samples were subjected to stress levels ranging from 5.1 to 9.2 MPa. Table 4.3 shows the failure time of samples during the crack propagation tests. The failure time is defined as the time required for the sample, having an initial crack, to separate apart into two halves when subjected to tensile load.

Table 4.2: Experimental condition during crack propagation (w = 3.2 cm)

Sample	**Carbonyl Index (CI)**	**Stress level (MPa)**	**Initial crack length/ Sample width (a/w)**
A	44	9.2	0.203
B	55	7.7	0.218
C	62	7.0	0.194
D	64	6.3	0.166
E	76	5.8	0.144
F	88	5.1	0.178
G	93	6.3	0.131

Table 4.3: Failure time of samples in crack propagation experiments

Sample	**Failure time (hrs)**
A	0.24
B	1.39
C	1.83
D	180.5
E	171.6
F	163.8
G	0.40

It was found that for the same level of degradation, the crack propagation rate increased with an increase in stress level. For samples D, E and F, with CI of 64, 76 and 88, respectively the failure time is more than 70 times longer than for samples A, B and C. This longer failure time can be attributed to smaller initial lengths of the crack in the samples D, E and F than in the samples A, B and C. The sample G with CI 93 has also smaller initial crack length but the sample is degraded to greater extent and the load is also high. Therefore, this sample did not show long failure time despite short initial crack length. The combined effect stress, crack length and degradation will be considered subsequently.

The crack propagation was recorded in a video and the crack length vs. time data were obtained. Figure 4.4 shows the crack length vs. time data for a sample degraded to a particular extent and subjected to certain level of stress.

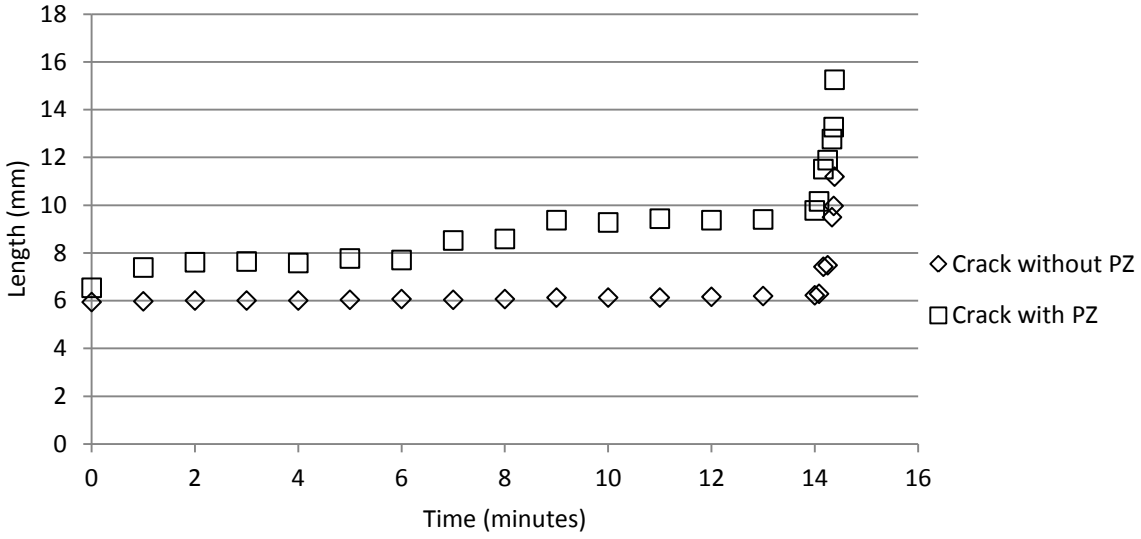

Figure 4.4: Crack and process zone vs. time at 9.2 MPa for a polymer sample having CI as 44

The rate of crack propagation and stress intensity factor were found by using equations 3.2 and 3.3. After obtaining the rate of crack propagation log (K) vs. log (da/dt) plots for samples degraded to different ranges and subjected to different stress levels were obtained as shown in Figure 4.5. K is expressed in $Pa\sqrt{m}$ and da/dt is expressed in m/s. The degradation level and the stress level during the test corresponding to the samples are provided in Table 4.2. The plot shows that as the crack propagates the crack speed increases. The crack propagation rate ranged from the order of 6.31×10^{-10} m/s to 1.26×10^{-2} m/s while the stress intensity factor ranged from the order of 0.91 $MPa\sqrt{m}$ to 4.07 $MPa\sqrt{m}$. The results data were classified according to the extent of degradation and

stress level into different groups and the effect of these factors on crack propagation was studied.

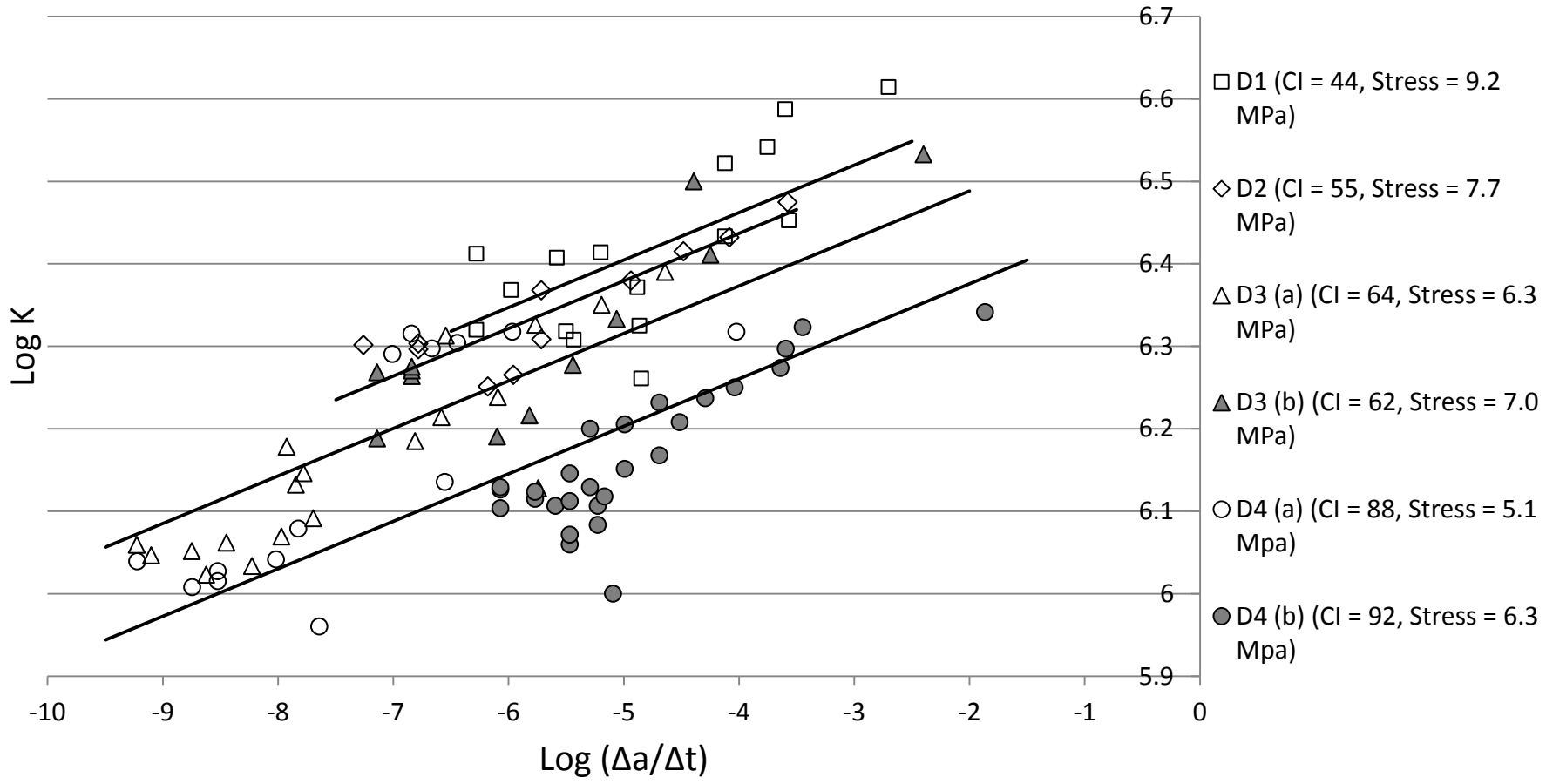

Figure 4.5: Results of crack propagation experiments conducted on HDPE plaque samples

4.2.1 Effect of Degradation on Crack Propagation

Figure 4.5 contrasts the crack propagation behavior of the polymer samples degraded to different degrees. The samples were divided into four groups D1, D2, D3 and D4 in their degradation order D1<D2<D3<D4. Except in terms of degradation level, the samples are same. The carbonyl index values are listed in Table 4.3. Groups D3 and D4 have been further divided into two parts: 'a' and 'b' corresponding to lower and higher stress levels. It can be noted that the region D1, which includes the curve for the least degraded sample, has the greatest log (K). The region D4, which includes the curves for most degraded samples, has the least log (K). Regions D2 and D3, which include the samples degraded to intermediate level, are between regions D1 and D4. The relationship between these regions indicates that as the degradation extent increases lower stress levels are required for crack propagation at the same rate.

Table 4.4: Carbonyl index for different groups

	D1	D2	D3(a)	D3(b)	D4(a)	D4(b)
Carbonyl index	44	55	62	64	88	93

4.2.2 Effect of Stresses on Crack Propagation

Figure 4.5 shows the four regions D1, D2, D3 and D4 of degradation as discussed earlier. In regions D3 and D4 there are two log (K) vs. log (da/dt) curves for two samples

which were degraded to almost same extent but subjected to different tensile loads. It was found that, in these regions, as the stress increases the rate of crack propagation increases.

For brittle materials, the rate of crack growth and stress intensity factor are related through the standard equation of linear elastic fracture mechanics (LEFM): $\frac{da}{dt} = CK^n$. To investigate whether this equation fits the data for degraded PE, lines were fitted to each of the four degradation levels' data sets in log(K) vs log(da/dt) plot. The exponent 'n', which relates to the slope in Figure 4.5 as slope = 1/n, was assumed to be independent of the degradation while 'C', which relates to intercept of the lines as intercept = - log(C)/n, was taken to be a function of degradation (represented by carbonyl index CI). The LEFM equation modifies to

$$\frac{da}{dt} = C(CI)K^n \quad . \qquad (4.1)$$

The fit was made through MATLAB programming. The best fit was decided on the basis of least sum of R squared values for each of the four sets. Procedure for obtaining the fit is given in detail in Appendix B.

The best fit average R-squared value was found to be 0.60. The intercepts of the fitted lines ranged from 6.49 to 6.69. The slope, intercept and corresponding CI to the different groups are shown in Table 4.5. R-squared values for degradation levels D1, D2, D3 and D4 were found to be 0.34, 0.88, 0.46 and 0.73, respectively. The best fit is obtained for degradation levels D2 and D4 corresponding to CI of 55 and 90 respectively. An alternate fitting approach, with only C as a function of degradation, was investigated.

The average R^2 value for this approach was also 0.60, with the best fit obtained for degradation levels D1 and D3. In this work, the approach in which the best fit is obtained for the most degraded samples (level D4) was selected for further study. From Table 4.5 it can be noted that as the level of degradation increases the intercept decreases. The intercept represents the stress level for a unit crack propagation rate. Thus, when the degradation is higher, a lower load is required for crack propagation. The intercepts of the lines fitted on log (K) vs. log (da/dt) data with the slope averaged for different groups were plotted with the average carbonyl index for each group as shown in Figure 4.6. The data were found to be linearly related such that

$$I = -0.0045(CI) + 6.9. \quad (4.2)$$

Table 4.5: Intercepts of trend line with average slope on the log (K) axis

Group	**Average CI**	**Slope**	**Intercept**	**R^2**
D1	44	0.058	6.69	0.34
D2	55	0.058	6.66	0.88
D3	63	0.058	6.60	0.46
D4	90	0.058	6.49	0.76

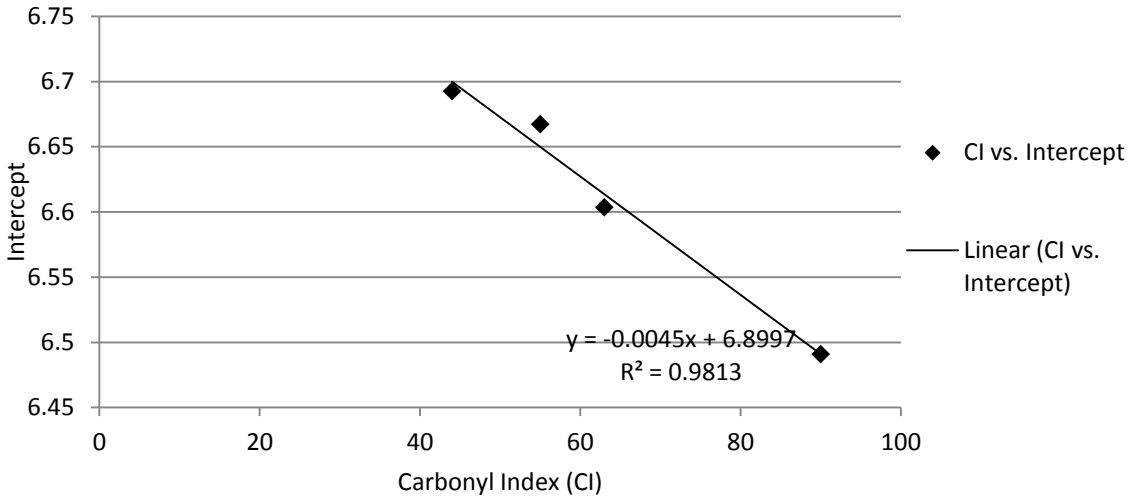

Figure 4.6: Intercept on log (K) axis vs. average degradation level (CI) for different groups

4.3 SEM RESULTS

SEM images of were obtained of a sample surface after completion of the crack propagation test. It was found that small cracks developed on the surface of the sample as shown in Figure 4.7. The cracks appear to be uniformly distributed on the surface although the length and width of the cracks vary. The cracks are oriented parallel to each other. Since there is no preferential direction associated with sample degradation, it can be inferred that the parallel orientation indicates that the cracks were created due to tension in the sample during the crack propagation test. Since other types of material failure, like void generation, were not observed on the surface, it seems very likely that these cracks are responsible for macroscopic cracks--the ultimate cause of polymer mechanical failure such as occurs in pipes.

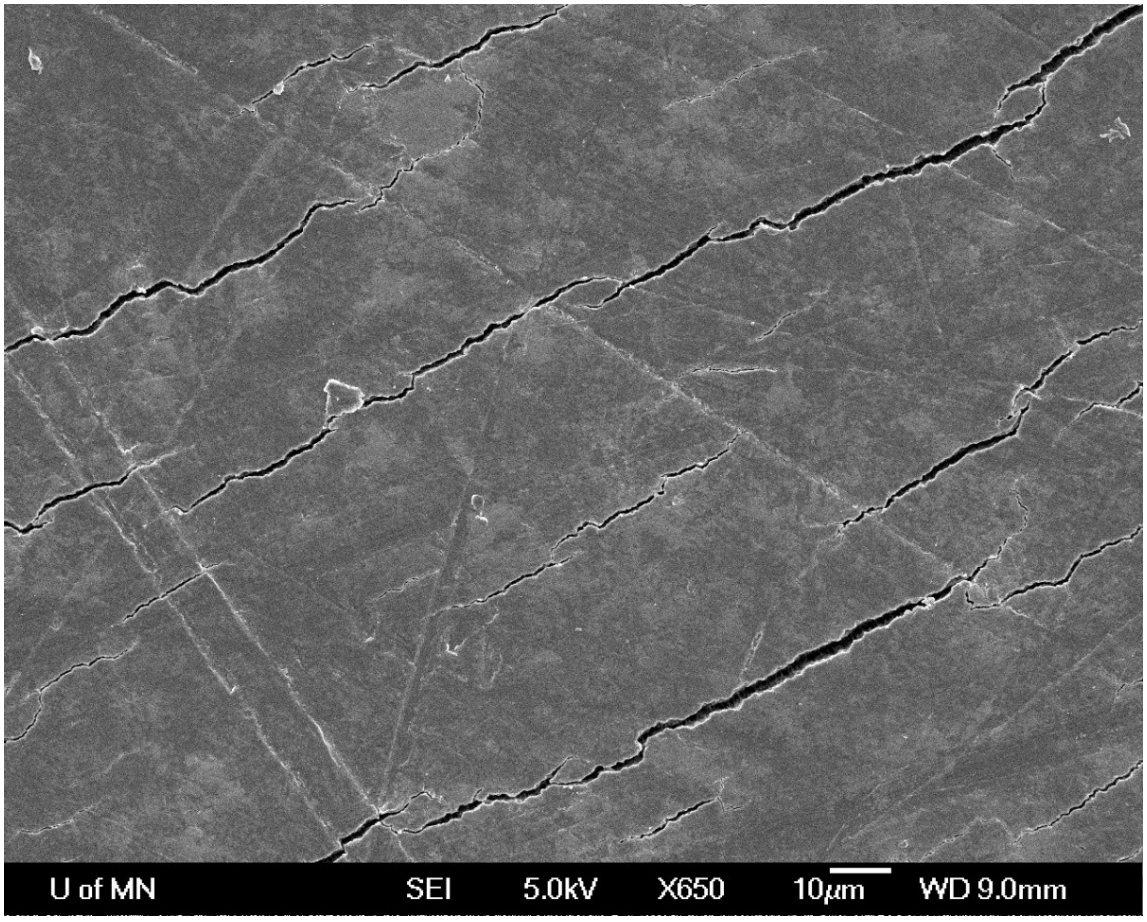

Figure 4.7: A SEM image of a HDPE plaque sample (CI = 44) showing micro cracks after completion of the crack propagation test

An SEM image of a microcrack under high magnification shows small fibers connecting the two inner surfaces of the crack (Figure 4.8). No deformation is noted in the bulk material adjacent to the fracture surface.. Even though the polymer had become brittle upon oxidation, the stretching of fibers indicates the presence of microlevel ductility in the material. The fiber stretching sheds light upon the crack initiation mechanism in high density polyethylene. From the fiber stretching it can be concluded

that the mechanism of failure involves the separation of material surfaces resulting in connecting fibers and voids. The fibers elongate with the separation of surfaces and ultimately break, resulting in generation of crack.

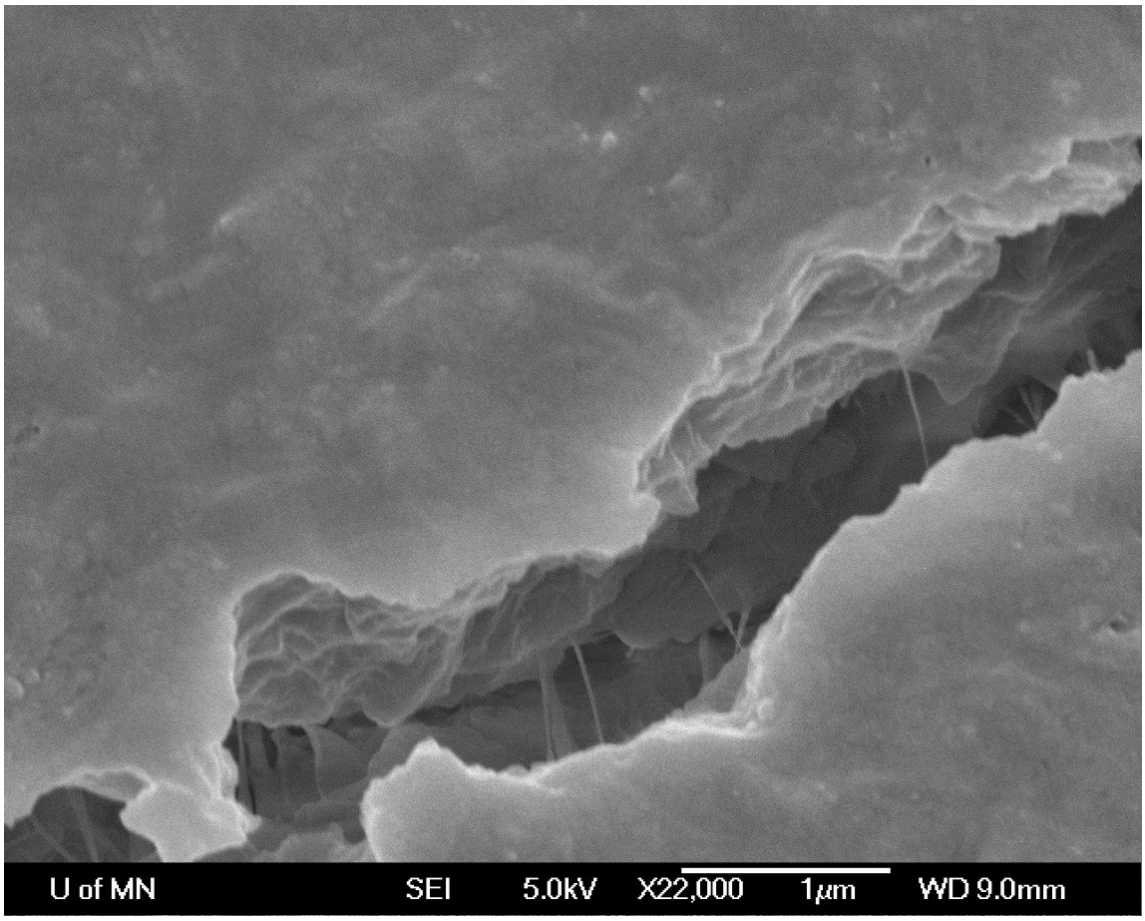

Figure 4.8: A SEM image of a HDPE plaque sample showing fibers inside a micro crack after completion of the crack propagation test

The edge of the broken sample, which contained the process zone, was also observed through SEM (Figure 4.9). Several fibers, which were stretched and broken, can be seen in the image. Within the process zone, a thin film of polymer is formed,

preceding the separation of the plaque sample into two halves. The process zone itself propagates through the fiber stretching and breaking mechanism. Additional SEM images can be found in Appendix C.

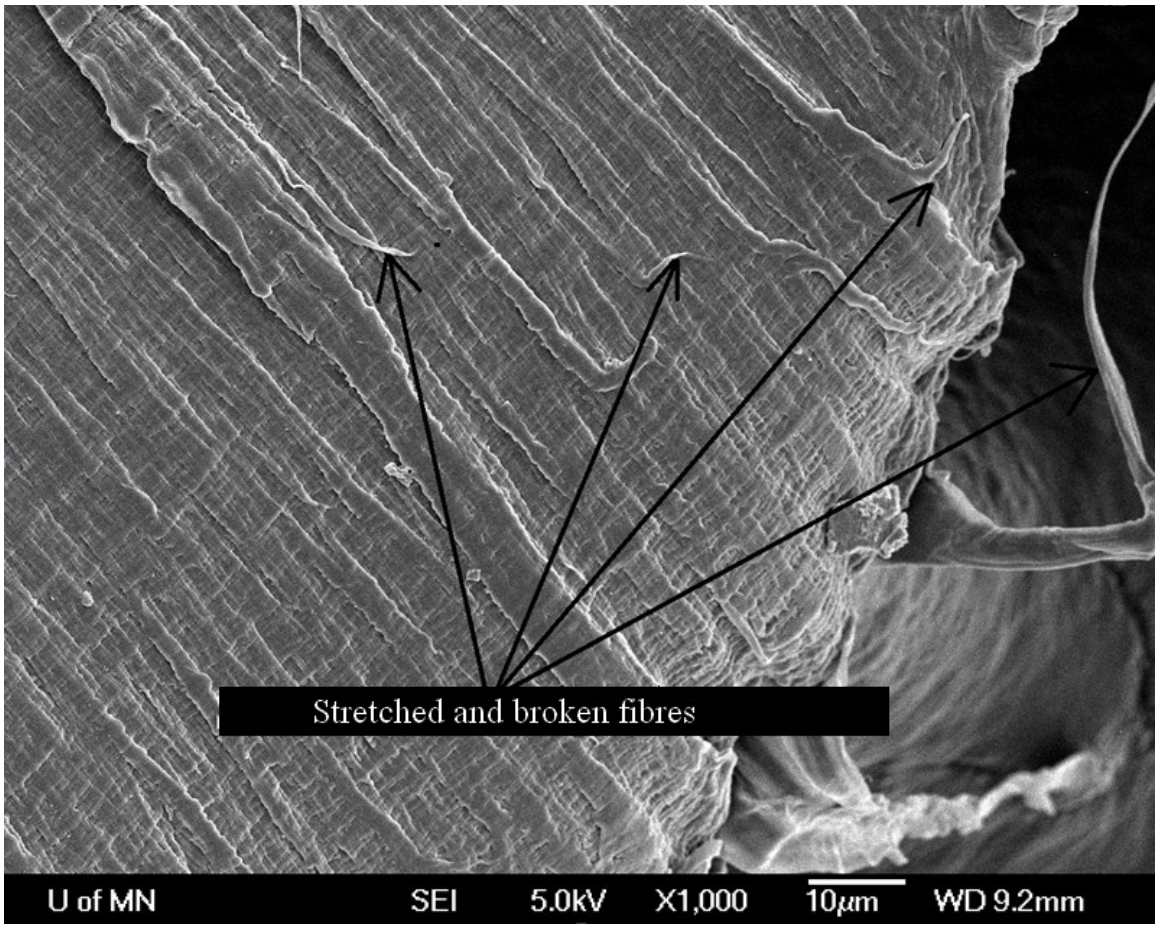

Figure 4.9: A SEM image of a HDPE plaque sample showing the crack edge after completion of the crack propagation test

5. APPLICATION TO LIFETIME PREDICTION

In this chapter a framework is presented to apply the results and findings of this work to applications in the polymer industry. This chapter presents an approach to predict lifetime of a thin tube with flowing potable water; the tube is assumed to be uniformly degraded through the thickness but the degradation varies with time. Results presented in chapter 4 are used to obtain the time for a crack to propagate through the thickness of the tube.

It was found in chapter 4 that the relationship between the crack propagation rate, stress level and degradation follow a form similar to LEFM:

$$\frac{da}{dt} = C(D)\, K^{n} \qquad (5.1)$$

where C(D) denotes that C is a function of degradation (D). In general a tube is non-uniformly degraded. So, D = D(x, t) where 'x' denotes position and t represents time. However, a thin tube immersed in an oxidative environment can be assumed to be uniformly degraded throughout the thickness. Therefore, for the thin tube case under consideration D = D(t). The parameter 'C' is therefore a function of time only so that C = C(t). The experimental data for degradation and crack growth from chapter 4 provide a methodology for obtaining C(t) by:

a) Establishing CI as a function of exposure time from FTIR data. Figure 4.2 shows a linear relationship such that $CI = C_1t + C_2$ where C_1 and C_2 are constants,

b) Establishing the intercept (I) as a function of CI from crack propagation data. It was found from the experimental work that intercept is related to CI as:

I = -0.0045(CI) +6.9. The intercept I is related to C as I = -(log C)/n. Thus, 'C' can be obtained as a function of time.

Therefore, equation (5.1) can be written as:

$$\frac{da}{dt} = C(t)K^n \quad . \qquad (5.2)$$

Substituting $K = Y\sigma\sqrt{(\Pi a)}$ in equation 5.2

$$\frac{da}{dt} = C(t)(Y\sigma\sqrt{(\Pi a)})^n \qquad (5.3)$$

is obtained. The geometric factor 'Y' is a function of crack length and an empirical expression of 'Y' can be obtained from a handbook of stress intensity factors. To evaluate the time for crack to propagate through the thickness of tube (t_f) equation 5.3 is integrated as:

$$\int_{a_o}^{a_{final}} \frac{1}{(Y\sigma\sqrt{\Pi a})^n} da = \int_0^{t_{final}} C(t)dt \qquad (5.4)$$

where $a_{final} = r_o - r_i$ (see Figure 5.1). The solution for equation 5.4 can be obtained either numerically or analytically and the time duration for the crack to propagate through the thickness of the tube can be evaluated.

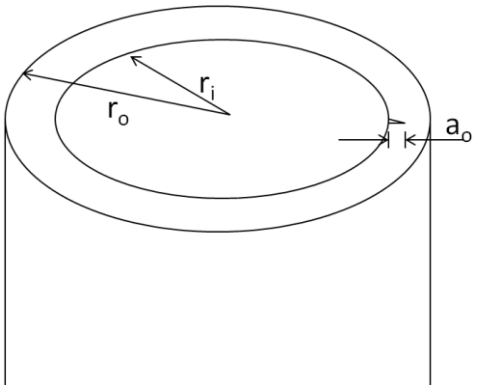

Figure 5.1: A sketch of a tube with an initial crack present at its inner surface

6. CONCLUSION AND RECOMMENDATIONS

6.1 CONCLUSION

Low cost polymer materials such as polyethylene are extensively used for pipe applications. In this application ultraviolet or chlorinated water exposure can lead to degradation of the polyethylene. In the study presented herein the HDPE samples were degraded to various extents by subjecting the material to 8 ppm chlorinated water at 80°C. These differently degraded samples represent the regions of varying degradation through the component thickness. Crack propagation behavior dependence on degradation and stress was characterized in the study. The experimental approach presented in this study is a novel way to understand the effect of both chemical degradation and the stresses on the crack propagation behavior in the HDPE films.

Specimens for crack propagation tests were prepared through exposure in chlorinated water which degrades the mechanical properties of polymer. The degradation of the sample was measured through FTIR spectroscopy in terms of Carbonyl Index (CI) values and also through tensile test by measure of the strain-at-failure. Because of the good correlation between FTIR, a non destructive technique, and strain-at-failure the extent of degradation in crack propagation samples was quantified by FTIR. Samples, degraded to four different levels, were prepared using FTIR and crack propagation tests, at a constant load, were conducted on the samples. During the tests, different samples

were subjected to different stress levels. The results helped in understanding the effect of degradation and stress levels on crack propagation behavior. As shown in Chapter 5, these results can be implemented in the form of a model which can be solved either analytically or numerically to predict crack propagation behavior and understand the effect of initial crack length, stress levels, and degradation rate on crack propagation.

Four ranges of CI were identified corresponding to the extent of degradation: level 1 with CI 35–50, level 2 with CI 50–65, level 3 with CI 65–80, and level 4 with CI 80–100 were prepared. It was found that the strain-at-failure decreased sharply with the increase in CI. A non-degraded sample showed the strain-at-failure value of about 7 while a degraded sample with CI value of 53.6 showed strain-at-failure of 0.15. Thus higher CI indicates more degraded material. A strong power law relationship, with R squared value of 0.88, was found to exist between the carbonyl index values of degraded samples and their strain-at-failure property. Thus, FTIR spectroscopy was established as a non destructive technique to quantify the degradation of mechanical properties of the polymer. The use of thin films of polymers for crack propagation tests provided the specific advantage of shorter degradation time.

The crack propagation tests were conducted on degraded samples with CI values ranging from 35 to 93. The samples were subjected to stresses ranging from 5.1 MPa to 9.2 MPa. The applicability of the Linear Elastic Fracture Mechanics (LEFM) approach was investigated: essentially the data were curve fit to a log relationship between rate of crack propagation and the stress intensity factor i.e. $\frac{da}{dt} = CK^n$. Crack propagation data for

samples, with similar degradation but subjected to a range of stress, could be fit with same LEFM equation. Thus, the data were fit by $\frac{da}{dt} = CK^n$ with C and n remaining constant for that level of degradation. Log (C) ranged from -112.7 to -116.2 when K (stress intensity factor) was expressed in units of $Pa\sqrt{m}$. If K is expressed in usual units of $MPa\sqrt{m}$ log (C) ranged from -12.0 to -8.5. For typical polymers log(C) ranges from -4 to -10. For different degradations levels all data sets follow the same slope (i.e. 1/n = 0.058, n=17.4) but the log (K) intercept is a function of degradation. 'C' increases exponentially with carbonyl index. For typical polymers 'n' is found to be about 3–4, however values up to 17 have been obtained [31] for polymethyl methacrylate (a relatively brittle polymer). The relative higher value of n, found in the present work, implies higher crack propagation speed which can be attributed to the brittle behavior of polymer caused by exposure to chlorinated water.

Also, SEM images of the surface of a sample used for crack propagation test show parallel orientation of the cracks in a direction perpendicular to stress. This indicates that there is a high probability that cracks were formed due to mechanical loading and not because of chemical degradation. Further investigation is needed to confirm this finding.

6.2 RECOMMENDATIONS FOR FUTURE WORK

In this study the carbonyl index, a FTIR spectroscopy parameter, was used as a chemical measure of degradation. The advantage of using FTIR was that it did not destroy the sample and the sample could be used for crack propagation test. Also, FTIR can distinguish between the degradation levels which cannot be differentiated using strain-at-failure. However, in the mid level of degradation (10-20 days of exposure) the data are insufficient to distinguish the degradation levels. More experimental data is needed in this range of degradation.

The LEFM model fit to the data was not uniformly consistent across degradation levels. Additional samples that would allow for either a double edged notch specimen or a center slit specimen are recommended. These sample geometries show less variation in the geometry factor (Y) and may lead to less variability in the crack growth data. In chapter 5 a framework has been proposed for predicting the life time of degraded polymer tubes using an LEFM approximation for crack growth. The temperature, initial crack length, geometry of the sample and chlorine concentration are some of the important factors which control the life time of the polymer structure and their effect should be investigated in the experimental work. Future studies should also consider other crack propagation modeling approaches that allow for ductile behavior in the process zone.

Fracture toughness of a material is another important property required for designing the structure because it determines the critical amount of loading that the

structure can sustain without failure. In the work presented herein on crack propagation, rate dependence on several factors have been considered. It would be quite interesting to study the dependence of fracture toughness on the degradation of the polymer. An understanding of the fracture toughness and the crack growth rate can make a significant impact on the design of the pipes which are installed for application in a degrading environment.

REFERENCES

1. High Performance PE Materials For Water Piping Applications, Muncipal and Industrial Division, Plastics Pipe Institute, TN-41/2007, 2007
2. R. K. Krishnaswamy, A. M. Sukhadia, M. J. Lamborn, Is Pent A True Indicator of PE Pipe Slow Crack Growth Resistance?, Chevron Phillips Chemical Company, Bulletin: PP 818-TN
3. M.F. Kanninen, P.E. O'Donoghue, C. H. Popelar, and V.H. Kenner, A Viscoelastic Fracture Mechanics Assessment of Slow Crack Growth in Polyethylene Gas Distribution Pipe Materials, Engineering Fracture Mechanics, 36(6), 903 – 918, (1990)
4. N. Brown, Slow Crack Growth – Notches – Pressurized Polyethylene Pipes, Polymer Science and Engineering, 47(11), 1951-1955, (2007)
5. Jana Laboratories Inc., Impact of Potable Water Disinfectants on PE Pipe, June 30, 2010
6. A. Frank, W. Freimann, G. Pinter, R. W. Lang, A Fracture Mechanics Concept for the Accelerated Characterization of Creep Crack Growth in PE – HD Pipe Grades, Engineering Fracture Mechanics, 76(18), 2780-2787, (2009)
7. U. Andersson, Which Factors Control the Lifetime of Plastic Pipes and How the Lifetime can be Extrapolated, Bodycote Polymer AB
8. The Plastics Pipe Institute, Inc., Rate Process Method for Projecting Performance of Polyethylene Piping Components TN – 16/99, (1999)
9. R. P. Brown, Handbook of Polymer Testing: Physical Methods, Marcel Dekker Inc., 339 – 340, (1999), ISBN 0-8247-0171-2
10. ASTM F1473-11. Retrieved 05/20, 2011, from http://www.astm.org.proxy2.library.illinois.edu/Standards/F1473.htm
11. ISO 13479:2009. Retrieved 05/20, 2011, from http://www.iso.org/iso/iso_catalogue/catalogue_ics/catalogue_detail_ics.htm?csnumber=45812

12. ISO 13479:1997. Retrieved 05/20, 2011, from http://www.iso.org/iso/catalogue_detail.htm?csnumber=22078
13. Testing method. Retrieved 05/20, 2011, from http://www.pe100plus.net/index.php/en/content/index/id/37
14. G. Pinter, R. W. Lang, and M. Haager, A Test Concept for Lifetime Prediction of Polyethylene Pressure Pipes, Monatshefte Fur Chemie,138, 347 – 355, (2007)
15. A. Frank, G. Pinter, and R. W. Lang, Accelerated Investigation of Creep Crack Growth in Polyethylene Pipe Grade Materials by The Use of Fatigue Tests on Crack Round Bar Specimens, Technical Paper, Regional Technical Conference – Society of Plastic Engineers 4, 2418 – 2422, (2008)
16. B.H. Choi, A. Chudnovsky, R. Paradkar, W. Michie, Z. Zhou and P. M. Cham, Experimental and theoretical investigation of stress corrosion crack (SCC) growth of polyethylene pipes, Polymer Degradation and Stability, 94, 859 – 867, (2009)
17. A. Chudnovsky, Crack Layer Theory, NASA Contractor Report 174634
18. N. Brown and X. Lu, A Fundamental Theory for Slow Crack Growth in Polyethylene, Polymer, 36(3), 543-548, (1995)
19. X. Lu and N. Brown, The Ductile – Brittle Transition in a Polyethylene Copolymer, Journal of Materials Science, 25, 29 – 34, (1990)
20. M. Lundback, Long – Term Performance of Polyolefins in Different Environments Including Chlorinated Water: Antioxidant Consumption and Migration, and Polymer Degradation, Thesis, KTH, Sweden
21. J.P. Dear and N.S. Mason, Effect of Chlorine on Polyethylene Pipes in Water Distribution Networks, 220 (L), J. Materials: Design and Applications, , 220(3), 97-111, (2006)
22. X. Lu, R. Qian, N. Brown, Discontinuous Crack Growth in Polyethylene Under a Constant Load, Journal of Materials Science, 26, 917 – 924, (1991)
23. B. Leis, T. Forte, J. Ahmad, M. Wilson, R. Kurth, P. Vieth and C. Cundiff, Investigation of the validity of the slow crack growth test, Topical Report, FRI Report No. 88/0131, Battelle Columbus Division for the Gas Research Institute (1988)

24. H.B.H. Hamouda, L. Laiarinandrasana and R. Piques, Fracture mechanics global approach concepts applied to creep slow crack growth in a medium density polyethylene (MDPE) Engineering Fracture Mechanics, 74, 2187-2204, (2007)
25. T. Trankner, M. Hedenqvist, and U.W. Gedde, Structure and Crack Growth in Gas Pipes of Medium – Density and High – Density Polyethylene, 36(16), 2069-2076, Polymer Engineering and Science, (1996)
26. J. A. Hingley and S. L. Mings, Fracture toughness of polyimide films, Polymer, 31(1), 75 – 77, (1990)
27. B. M. Klemann and T. DeVilbiss, The Fracture Toughness of Thin Polymeric Films, Polymer Engineering and Science, 36(1), 126 – 134, (1996)
28. M. K. V. Chan and J. G. Williams, Polymer, Slow Stable Crack Growth in High Density Polyethylenes, Polymer, 24, 234 – 244 (1983)
29. W. Camisa, S.C. Mantell, J. H. Davidson and G. Singh, Prediction of degradation of polyolefins used in solar domestic hot water components, Proceedings of ASME 2010 4th International Conference on Energy Sustainability, Phoenix, Arizona, USA, May 17-22, (2010)
30. W. Camisa, Antioxidant Loss in Polyethylene Exposed to Chlorinated Water, MS Thesis, University of Minnesota, 2009
31. G. P. Marshall, L. H. Coutts and J. G. Williams, Temperature Effects in Fracture of PMMA, Journal of Material Science, 9, 1409 – 1419, (1974)

APPENDIX A: CRACK LENGTH VS. TIME PLOTS

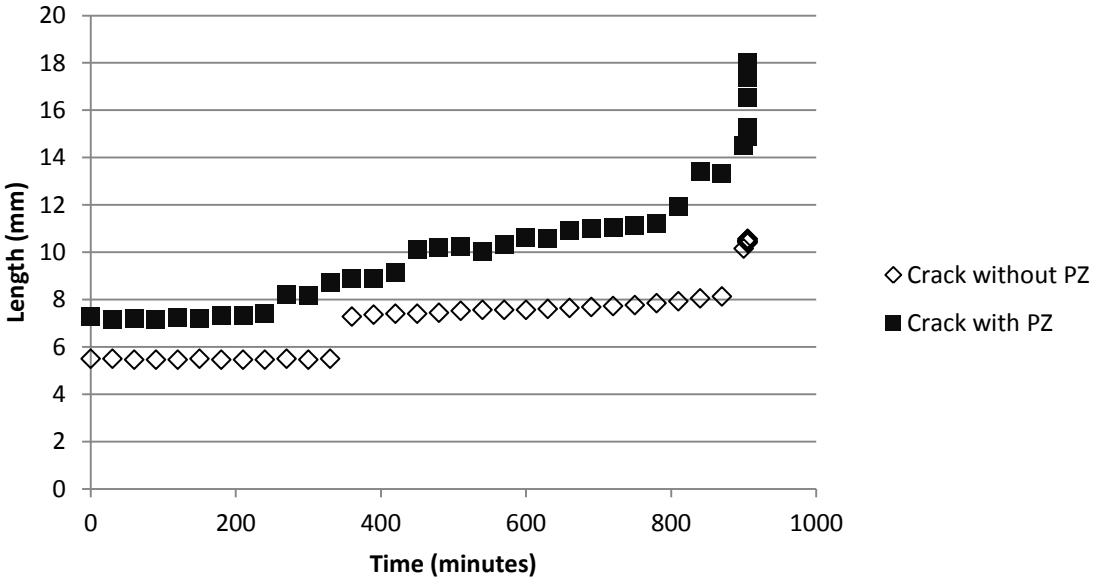

Figure A. 1: Crack length vs. time for a plaque HDPE sample having CI as 35.48 at a load of 7.7 MPa

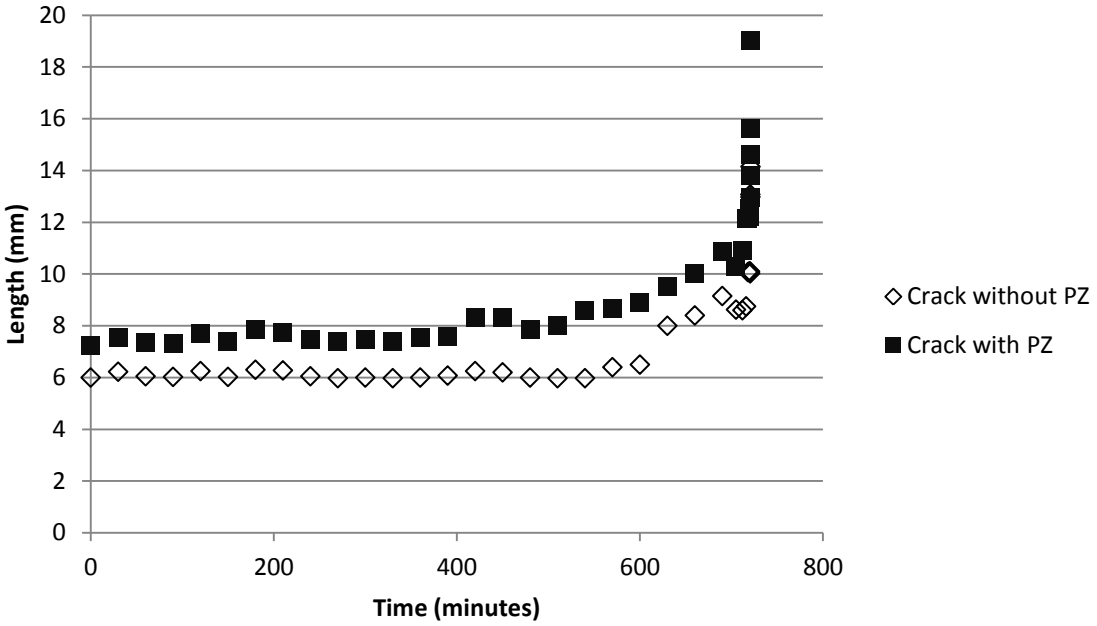

Figure A. 2: Crack length vs. time for a plaque HDPE sample having CI as 41.38 at a load of 6.3 MPa

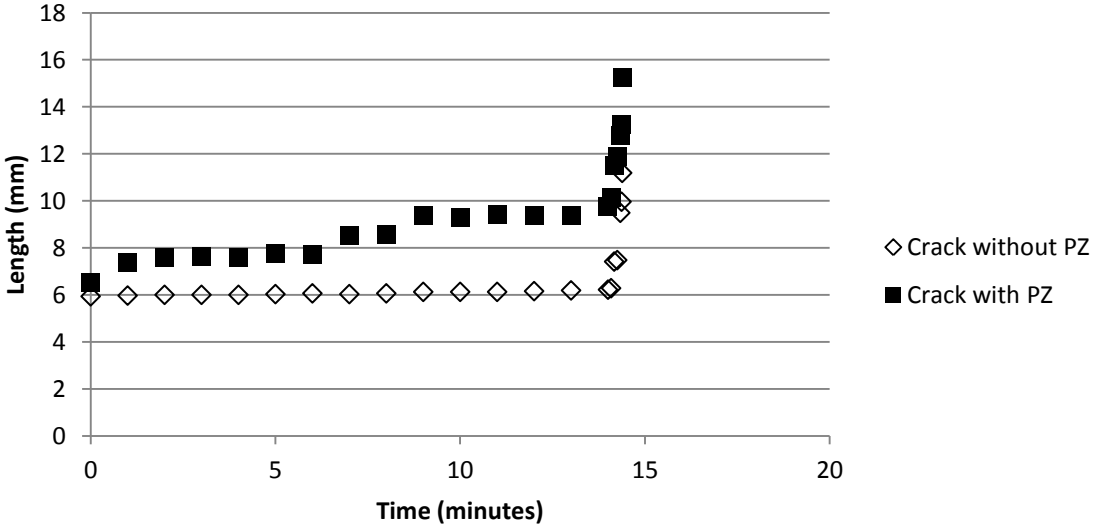

Figure A. 3: Crack length vs. time for a plaque HDPE sample having CI as 43.97 at a load of 9.2 MPa

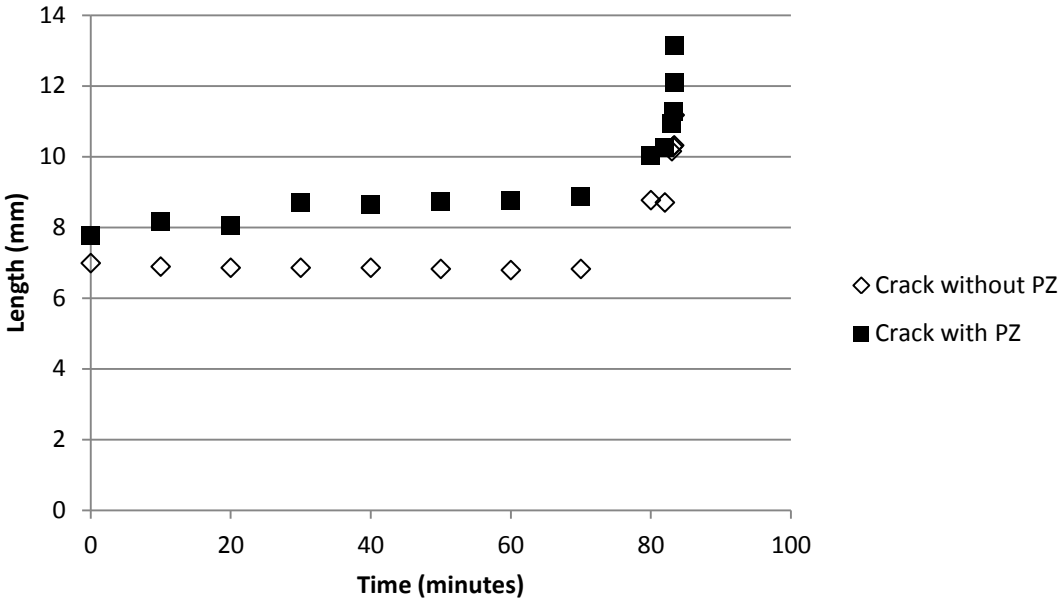

Figure A. 4: Crack length vs. time for a plaque HDPE sample having CI as 55.46 at a load of 7.7 MPa

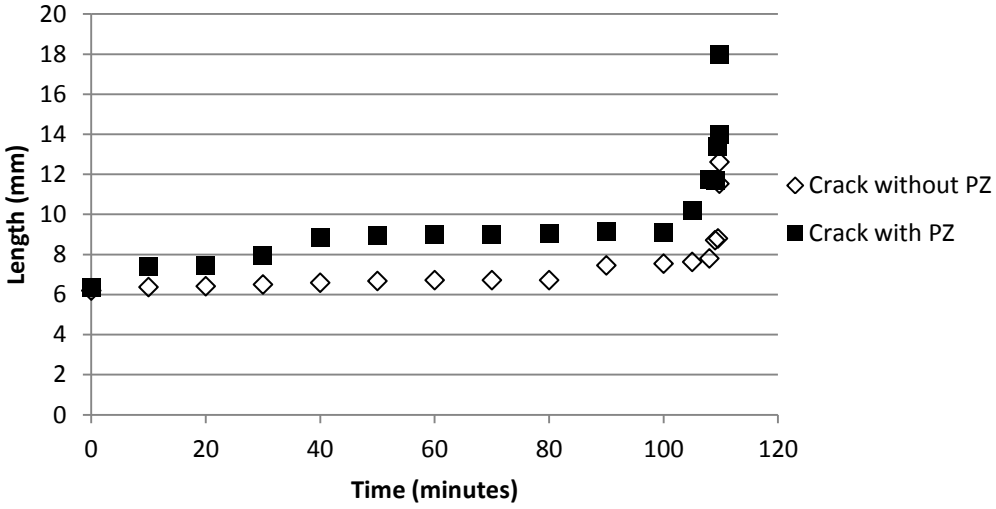

Figure A. 5: Crack length vs. time for a plaque HDPE sample having CI as 62.20 at a load of 6.96 MPa

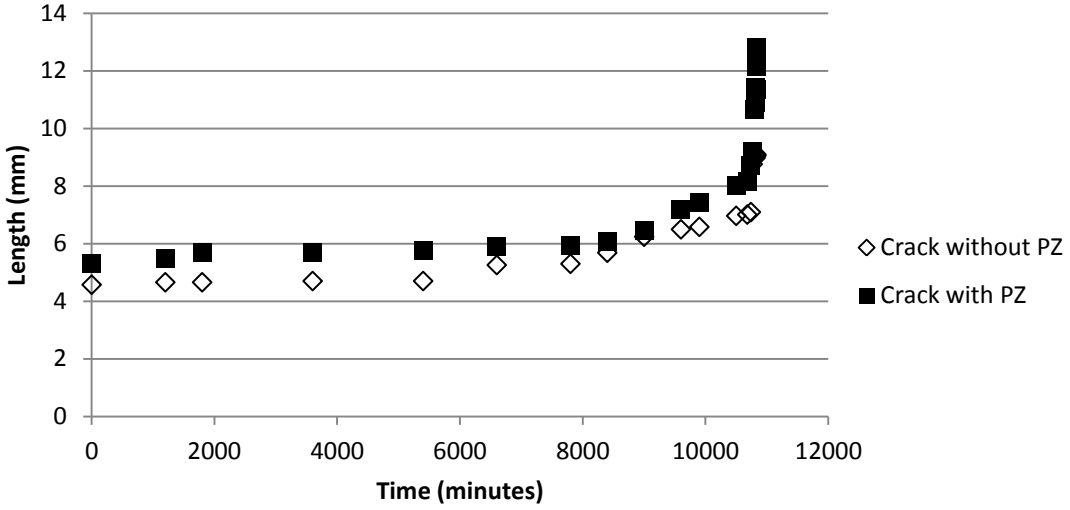

Figure A. 6: Crack length vs. time for a plaque HDPE sample having CI as 63.89 at a load of 6.3 MPa

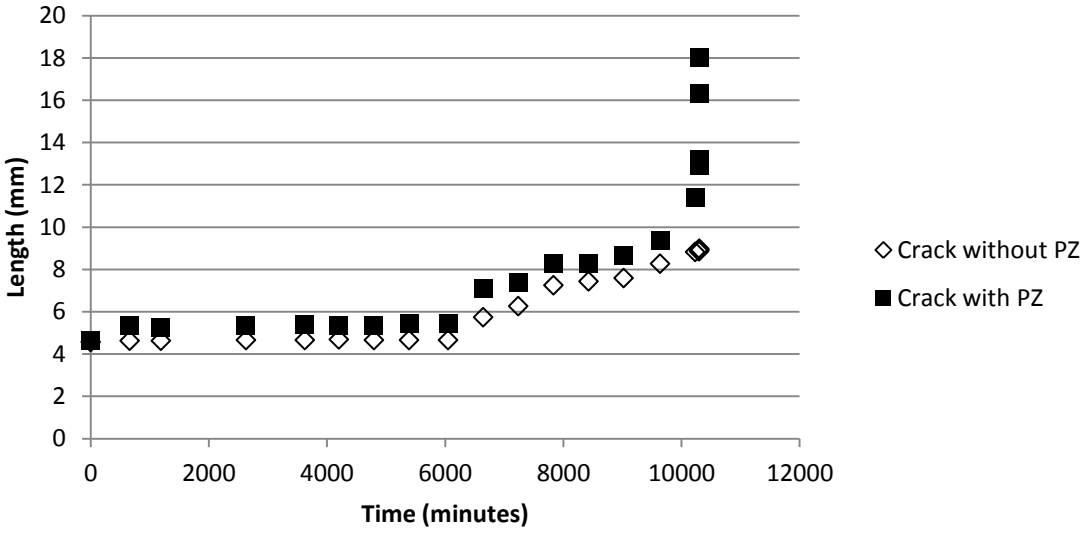

Figure A. 7: Crack length vs. time for a plaque HDPE sample having CI as 75.98 at a load of 5.8 MPa

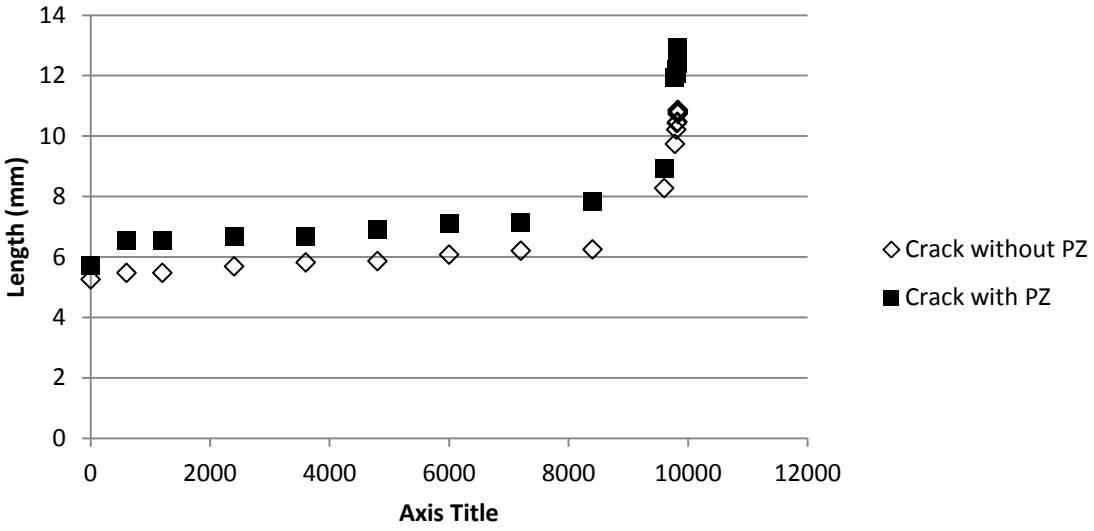

Figure A. 8: Crack length vs. time for a plaque HDPE sample having CI as 88.16 at a load of 5.1 MPa

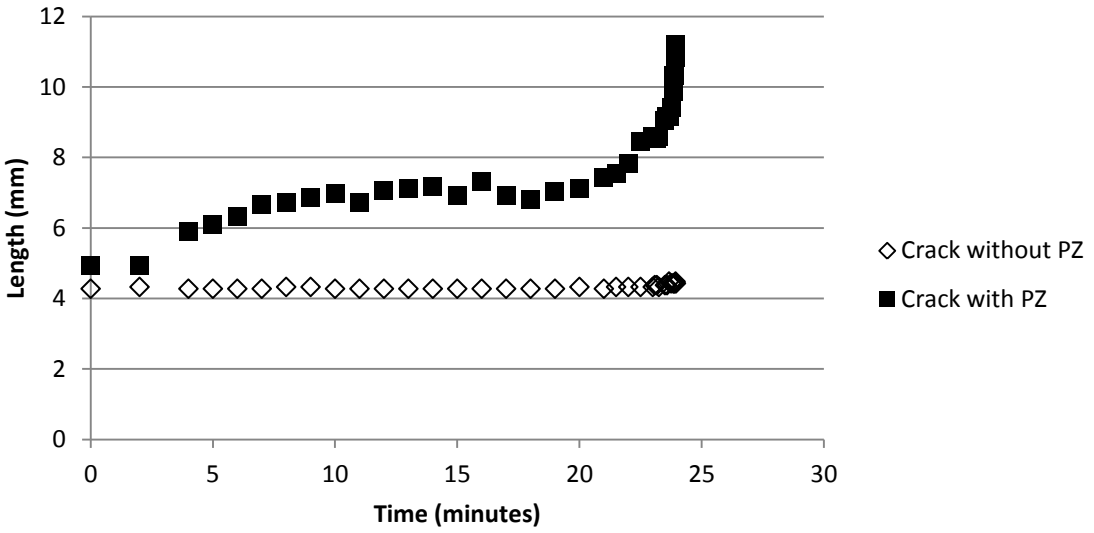

Figure A. 9: Crack length vs. time for a plaque HDPE sample having CI as 92.73 at a load of 6.3 MPa

APPENDIX B: CURVE FITTING

The intercepts and slope of the data presented in figure 4.6 were found using the ordinary least square method of linear algebra. The original equation relating the data (log (da/dt) and log(K)) is:

$$\log(da/dt) = n\log(K) + \log(C)$$

This equation of the line fit can be expressed in the matrix form as:

$$Y = X\beta + \epsilon$$

where $\beta = [C_1\ C_2\ C_3\ C_4\ n]$
C_n : intercept of the line fit of n^{th} group (based on degradation) on log(K) axis
n: slope of the line fit
ϵ: matrix of error difference between the experimental data and the predicted value

$$\epsilon = Y - X\beta$$

For minimizing error the sum of squared errors is minimized.

Sum of squared errors is given as:
$$\epsilon'\epsilon = (Y - X\beta)'(Y - X\beta) = Y'Y - 2Y'X\beta + X'X\beta$$

Differentiating $\epsilon'\epsilon$ with respect to β for minima we obtain

$$\beta = (X'X)^{-1}X'Y$$

APPENDIX C: SEM RESULTS

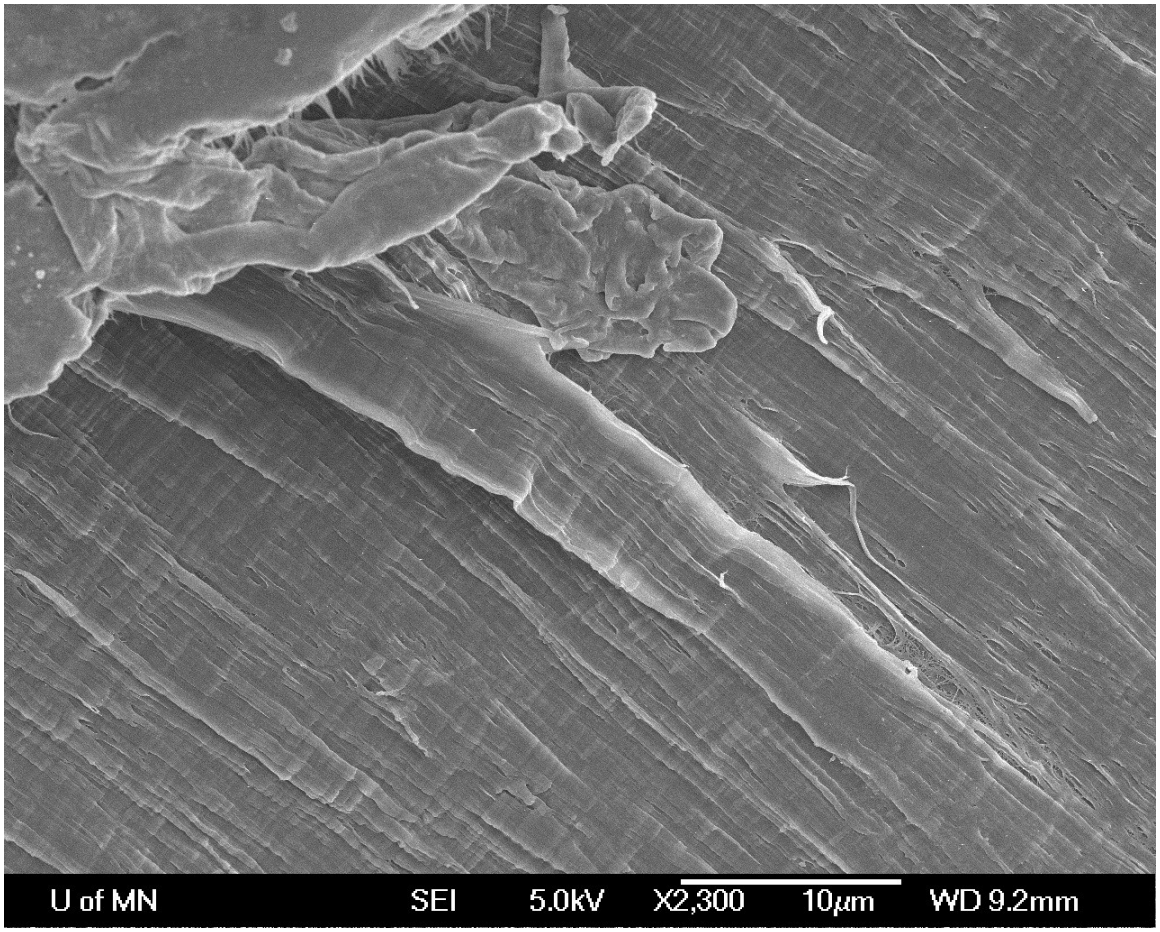

Figure C. 1: A SEM image of a HDPE plaque sample showing the process zone after completion of the crack propagation test

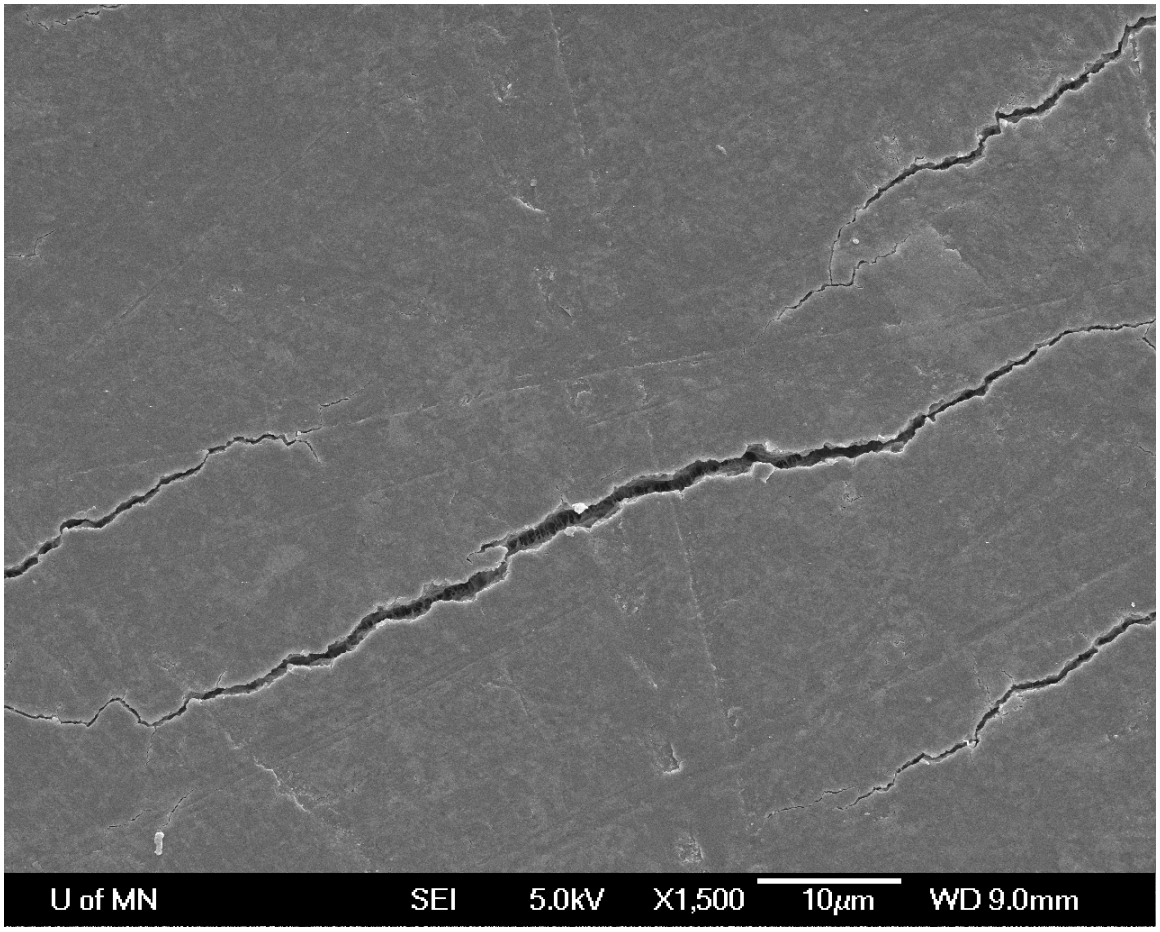

Figure C. 2: A SEM image of a HDPE plaque sample showing a micro crack after completion of the crack propagation test

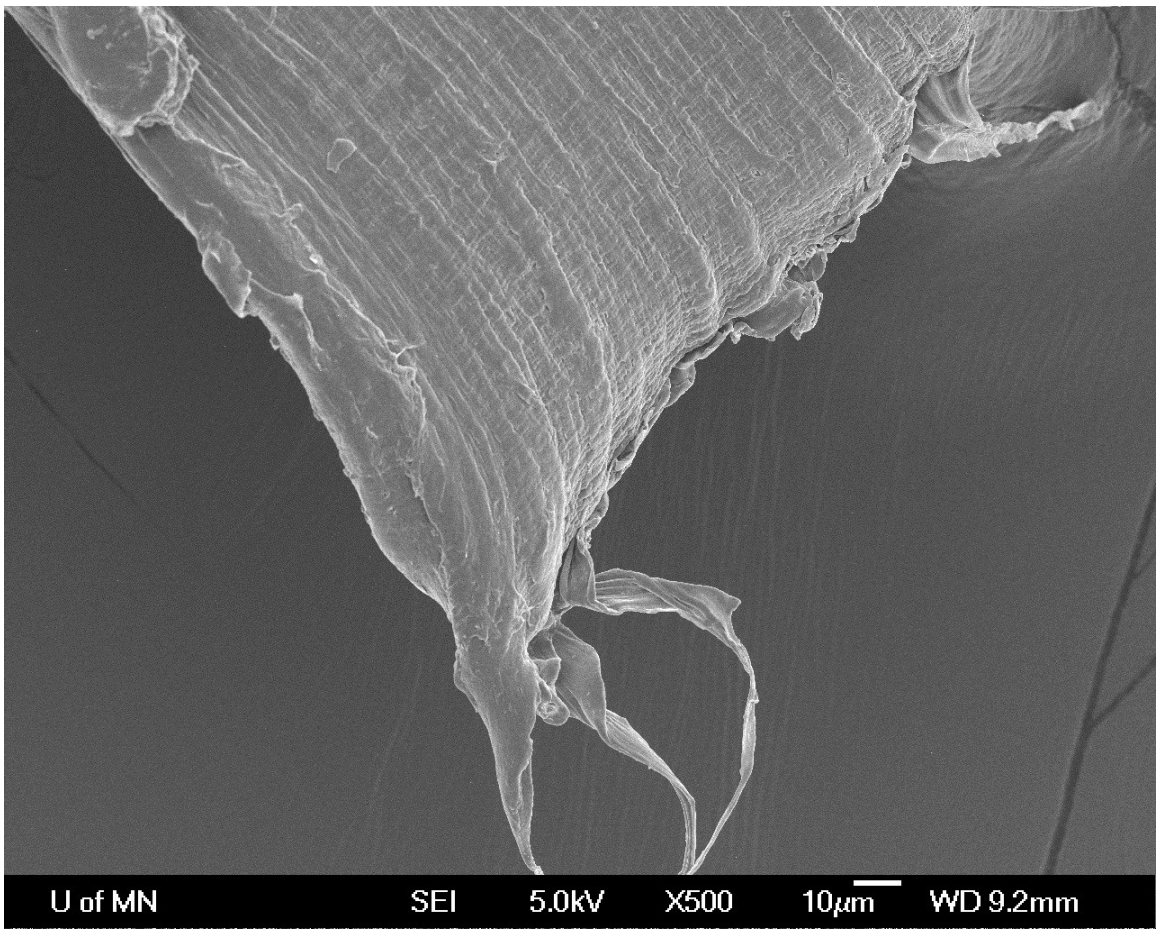

Figure C. 3: A SEM image of a HDPE plaque sample showing the edge part of the half broken part after completion of the crack propagation test

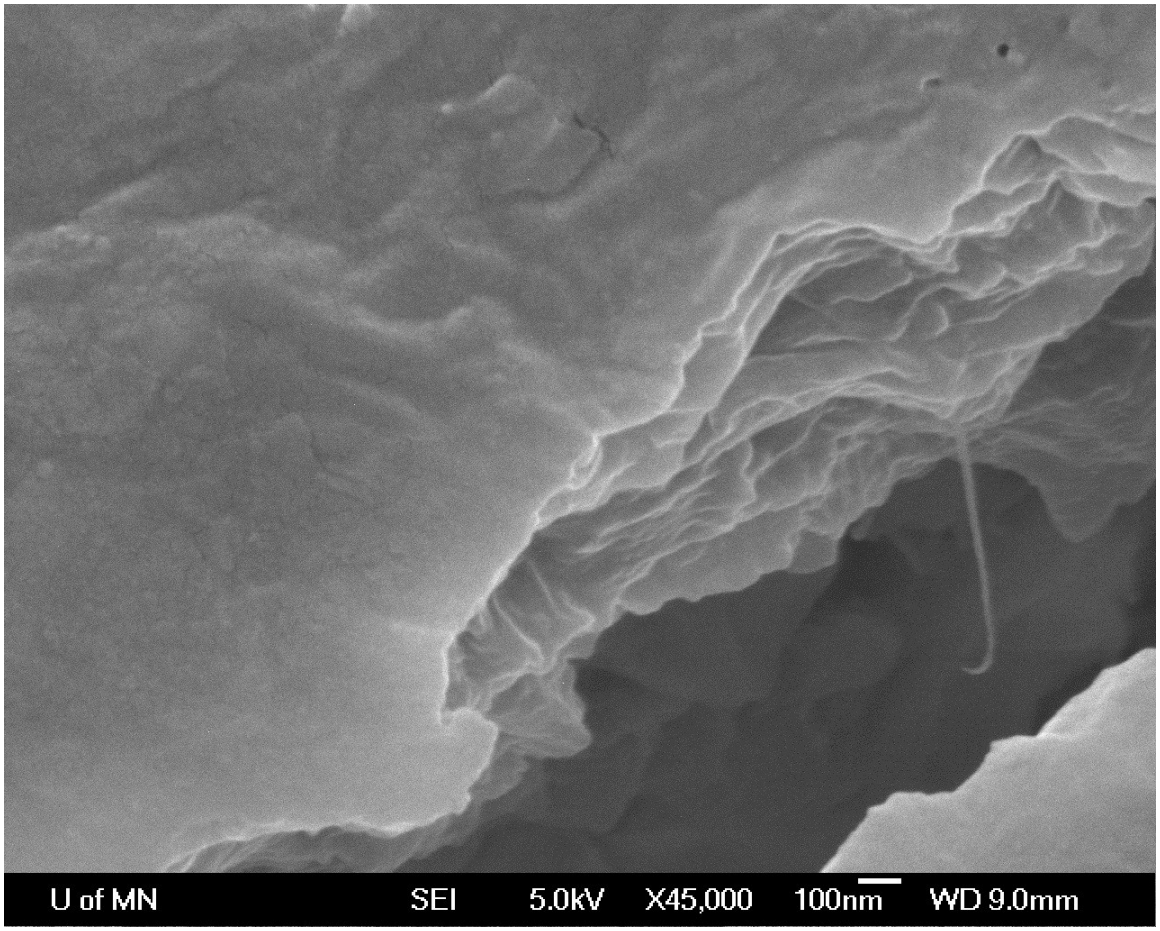

Figure C. 4: A SEM image of a HDPE plaque sample showing the inner surface of a micro-crack after completion of the crack propagation test